CROPPABLE KNOWLEDGE GRAPH EMBEDDING

Anonymous authors
Paper under double-blind review

ABSTRACT

Knowledge Graph Embedding (KGE) is a common method for Knowledge Graphs (KGs) to serve various artificial intelligence tasks. The suitable dimensions of the embeddings depend on the storage and computing conditions of the specific application scenarios. Once a new dimension is required, a new KGE model needs to be trained from scratch, which greatly increases the training cost and limits the efficiency and flexibility of KGE in serving various scenarios. In this work, we propose a novel KGE training framework MED, through which we could train once to get a croppable KGE model applicable to multiple scenarios with different dimensional requirements, sub-models of the required dimensions can be cropped out of it and used directly without any additional training. In MED, we propose a mutual learning mechanism to improve the low-dimensional sub-models performance and make the high-dimensional sub-models retain the capacity that low-dimensional sub-models have, an evolutionary improvement mechanism to promote the high-dimensional sub-models to master the knowledge that the low-dimensional sub-models can not learn, and a dynamic loss weight to balance the multiple losses adaptively. Experiments on 4 KGE models over 4 standard KG completion datasets, 3 real application scenarios over a real-world large-scale KG, and the experiments of extending MED to the language model BERT show the effectiveness, high efficiency, and flexible extensibility of MED. The code and data are available at `https://anonymous.4open.science/r/MED-DBFC/`.

1 INTRODUCTION

Knowledge Graphs (KGs) are composed of triples representing facts in the form of (*head entity, relation, tail entity*), abbreviated as (*h, r, t*). KG has been widely used in recommendation systems Zhu et al. (2021); Zhang et al. (2021), information extraction Hoffmann et al. (2011); Daiber et al. (2013), question answering Zhang et al. (2016); Diefenbach et al. (2018) and other tasks. A common way to apply a knowledge graph is to represent the entities and relations in the knowledge graph into continuous vector spaces, called knowledge graph embedding (KGE) Bordes et al. (2013); Sun et al. (2019b), and then use the vector representation of entities and relations to serve a variety of tasks.

KGEs with higher dimensions have greater expressive power and usually achieve better performance, but this also means a larger number of parameters and requires more storage space and computing resources Zhu et al. (2022); Sachan (2020). The appropriate dimensions of the KGE are different for different devices or scenarios. As shown in Fig. 1, large remote servers have large storage space and sufficient computing resources to support high-dimensional KGE with good performance, while small and medium-sized terminal devices, such as vehicle-mounted systems or smartphones, can only accept low-dimensional KGE due to limited computing power and storage capacity. Therefore, according to the conditions of different devices or scenes, people tend to train the KGE with appropriate dimensions and as high quality as possible. However, the challenge is that once a new dimension is required, a new KGE needs to be trained from scratch. Especially when only low-dimensional KGE can be applied, to ensure good performance, the additional model compression technology such as knowledge distillation Hinton et al. (2015); Zhu et al. (2022) is needed during training. This significantly increases training costs and limits KGE's efficiency and flexibility in serving different scenarios.

Thus a new concept "croppable KGE" is proposed and we are interested in the research question that **is it possible to train a croppable KGE, with which KGEs of various required dimensions can**

be cropped out of it, directly be used without any additional training, and achieve promising performance?

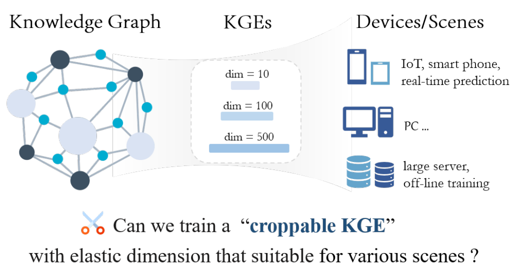

Figure 1: Diverse KGE dimensions for a KG.

In this work, our main idea of croppable KGE learning is to train an entire KGE that contains many sub-models of different dimensions in it. These sub-models share their embedding parameters and are trained simultaneously. The goal is that the low-dimensional sub-models can benefit from the more expressive high-dimensional sub-models, while the high-dimensional sub-models retain the ability of the low-dimensional sub-models and master the knowledge that the low-dimensional sub-models cannot. Based on this idea, we propose a croppable KGE training framework **MED**, which consists of three main modules, the **M**utual learning mechanism, the **E**volutionary improvement mechanism, and the **D**ynamic loss weight to achieve the above purpose. Specifically, the **mutual learning mechanism** is based on knowledge distillation and it makes pair-wise neighbor sub-models learn from each other, so that the performance of the lower-dimensional sub-model can be improved, and the higher-dimensional sub-model can retain the ability of the lower-dimensional sub-model. The **evolutionary improvement mechanism** helps the high-dimensional sub-model master more knowledge that the low-dimensional sub-model cannot by making the high-dimensional sub-model pay more attention to learn the triples that the low-dimensional sub-model can't correctly predict. The **dynamic loss weight** is designed to adaptively balance multiple losses of different sub-models according to their dimensions and further improve the overall performance.

We evaluate the effectiveness of our proposed MED by implementing it on three typical KGE methods and four standard KG datasets. We also prove its practical value by applying MED to a real-world large-scale KG and downstream tasks. Furthermore, we demonstrate the extensibility of MED by implementing it on language model BERT Devlin et al. (2019) and GLUE Wang et al. (2019) benchmarks. The experimental results show that (1) MED successfully trains a croppable KGE model available for various dimensional requirements, which contains multiple parameter-shared sub-models of different dimensions that of high performance and can be used directly without additional training; (2) the training efficiency of MED is far higher than that of independently training multiple KGE models of different sizes or obtaining them by knowledge distillation. (3) MED can be flexibly extended to other neural network models besides KGE and achieve good performance; (4) our proposed mutual learning mechanism, evolutionary improvement mechanism, and dynamic loss weight are effective and necessary for MED to achieve overall optimal performance. In summary, our contributions are as follows:

- We propose a new research question and task: training croppable KGE, from which KGEs of different dimensions can be cropped and used directly without any additional training.
- We propose a novel framework MED, including a mutual learning mechanism, an evolutionary improvement mechanism, and a dynamic loss weight, to ensure the overall performance of all sub-models during training the croppable KGE.
- We experimentally prove that all sub-models of MED work well, especially the performance of the low-dimensional sub-models exceeding the KGE with the same dimension trained by the state-of-the-art distillation-based methods. MED also shows excellent performance in real-world applications and good extensibility on other types of neural networks.

2 Related Work

This work is to achieve a croppable KGE that meets different dimensional requirements. One of the most common methods to obtain a good-performance KGE of the target dimension is utilizing knowledge distillation with a high-dimensional powerful teacher KGE. Thus, we focus on two research fields most relevant to our work: knowledge graph embedding and knowledge distillation.

2.1 Knowledge Graph Embedding

Knowledge graph embedding (KGE) technology has been widely applied with the key idea of mapping entities and relations of a KG into continuous vector spaces as vector representations, which can further serve various KG downstream tasks. TransE Bordes et al. (2013) is the most representative translation-based KGE method by regarding the relation as a translation from the head to tail entity. Variants of TransE include TransH Wang et al. (2014), TransR Lin et al. (2015), TransD Ji et al. (2015) and so on. RESCAL Nickel et al. (2011) is the first one based on vector decomposition, and then to improve it, DistMult Yang et al. (2015), ComplEx Trouillon et al. (2016), and SimplE Kazemi & Poole (2018) are proposed. RotatE Sun et al. (2019b) is a typical rotation-based method that regards the relation as the rotation between the head and tail entities. QuatE Zhang et al. (2019) and DihEdral Xu & Li (2019) work with a similar idea. PairRE Chao et al. (2021) uses two relation vectors to project the head and tail entities into an Euclidean space to encode complex relational patterns. With the development of neural networks, KGEs based on graph neural networks (GNNs) Dettmers et al. (2018); Nguyen et al. (2018); Schlichtkrull et al. (2018); Vashishth et al. (2020) are also proposed. Although the KGEs are simple and effective, there is an obvious challenge: In different scenarios, the required KGE dimensions are different, which depends on the storage and computing resources of the device. It has to train a new KGE model from scratch for a new dimension requirement, which greatly increases the training cost and limits the flexibility for KGE to serve diversified scenarios.

2.2 Knowledge Distillation

High-dimensional KGEs have strong expression ability due to the large number of parameters, but require a lot of storage and computing resources, and are not suitable for all scenarios, especially small devices. To solve this problem, a common way is to compress a high-dimensional KGE to the target low-dimensional KGE by knowledge distillation Hinton et al. (2015); Mirzadeh et al. (2020) and quantization Bai et al. (2021); Stock et al. (2021) technology.

Quantization replaces continuous vector representations with lower-dimensional discrete codes. TS-CL Sachan (2020) is the first work of KGE compression applying quantization. LightKG Wang et al. (2021a) uses a residual module to induce diversity among codebooks. However, quantization cannot improve the inference speed so it's still not suitable for devices with limited computing resources.

Knowledge distillation (KD) has been widely used in Computer Vision Mirzadeh et al. (2020) and Natural Language Processing Devlin et al. (2019); Sun et al. (2019a), helping reduce the model size and increase the inference speed. The core idea is to use the output of a large teacher model to guide the training of a small student model. DualDE Zhu et al. (2022) is a representative KD-based work to transfer the knowledge of high-dimensional KGE to low-dimensional KGE. It considers the mutual influences between the teacher and student and finetunes the teacher during training.MulDE Wang et al. (2021b) transfers the knowledge from multiple low-dimensional teacher models to a student model for hyperbolic KGE. ISD Zhou et al. (2022b) improves low-dimensional KGE by making it play the teacher and student roles alternatively during training. IterDE Liu et al. (2023) introduces an iterative distillation way and enables a KGE model to be the student and teacher during distilling alternately, thus knowledge can be transferred smoothly between high-dimensional teacher and low-dimensional student. Other distillation works related to knowledge graph include PMD Fan et al. (2024) applying distillation to pre-trained language models to improve KG completion, IncDE Liu et al. (2024) using distillation between the same-dimensional models at different times for incremental learning, and SKDE Xu et al. (2024) proposing self-knowledge distillation to avoid introducing a complex teacher model. Among these methods, DualDE Zhu et al. (2022) and IterDE Liu et al. (2023) are more relevant to our work, all have the setting that compresses high-dimensional teacher into low-dimensional student model. In this work, we propose a novel KD-based KGE training framework MED, one training can obtain a croppable KGE that meets multiple dimensional requirements.

3 Preliminary

Table 1: Score functions.

KGE method	Scoring Function $f(\mathbf{h}, \mathbf{r}, \mathbf{t})$
TransE Bordes et al. (2013)	$-\Vert\mathbf{h}+\mathbf{r}-\mathbf{t}\Vert$
SimplE Kazemi & Poole (2018)	$\frac{1}{2}(< h^H, r, t^T > + < t^H, r^{-1}, h^T >)$
RotatE Sun et al. (2019b)	$-\Vert\mathbf{h}\circ\mathbf{r}-\mathbf{t}\Vert$
PairRE Chao et al. (2021)	$-\left\Vert\mathbf{h}\circ\mathbf{r}^H-\mathbf{t}\circ\mathbf{r}^T\right\Vert$

Knowledge graph embedding (KGE) methods aim to express the relations between entities in a continuous vector space through a scoring function f. Specifically, given a knowledge graph $\mathcal{G} = (\mathcal{E}, \mathcal{R}, \mathcal{T})$ where $\mathcal{E}$, $\mathcal{R}$ and $\mathcal{T}$ are the sets of entities, relations and all observed triples, we utilize the triple scoring function to measure the plausibility of triples in the embedding space for a triple (h, r, t) where $h \in \mathcal{E}, r \in \mathcal{R}$ and $t \in \mathcal{E}$. The triple score function is denoted as $s_{(h,r,t)} = f(\mathbf{h}, \mathbf{r}, \mathbf{t})$ with embeddings of head entity $\mathbf{h}$, relation $\mathbf{r}$ and tail entity $\mathbf{t}$ as input. Table 1 summarizes the scoring functions of some popular KGE methods, where $\circ$ is the Hadamard product, $< x^1, ..., x^k >= \sum_i x_i^1 ... x_i^k$ is the generalized dot product. The higher the triple score, the more likely the model is to judge the triples as true. The optimization objective of KGE model is

$$L_{KGE} = - \sum_{(h,r,t) \in \mathcal{T} \cup \mathcal{T}^-} y \log \sigma(s_{(h,r,t)}) + (1-y) \log(1 - \sigma(s_{(h,r,t)})), \tag{1}$$

where $\mathcal{T}^- = \mathcal{E} \times \mathcal{R} \times \mathcal{E} \setminus \mathcal{T}$ is the set of negative triples, σ is the Sigmoid activation function, y is the ground-truth label of triple (h, r, t), $y = 1$ for positive triples and $y = 0$ for negative triples.

4 MED Framework

As shown in Fig. 2, our croppable KGE framework MED contains multiple (let's say n) sub-models of different dimensions in it, denoted as $M_i (i = 1, 2..., n)$ with dimension of d_i. Each sub-model M_i is composed of the first d_i dimensions of the whole embedding and the score of triple (h, r, t) output by M_i is $s^i_{(h,r,t)} = f(\mathbf{h}[0{:}d_i], \mathbf{r}[0{:}d_i], \mathbf{t}[0{:}d_i])$, where $\mathbf{h}[0{:}d_i]$ represents the first d_i elements of vector $\mathbf{h}$. The parameters of sub-model M_i are shared by all sub-models $M_j (i<j \leqslant n)$ that are higher-dimensional than it. The number of sub-models n and the specific dimension of each sub-model d_i can be set according to the actual application needs. For low-dimensional sub-models, we want to improve their performance as much as possible. For high-dimensional sub-models, we hope they cover the abilities that low-dimensional sub-models already have and master the knowledge that low-dimensional sub-models can not learn well, that is, they need to correctly predict not only the triples that low-dimensional sub-models can predict correctly but also those low-dimensional sub-models predict wrongly.

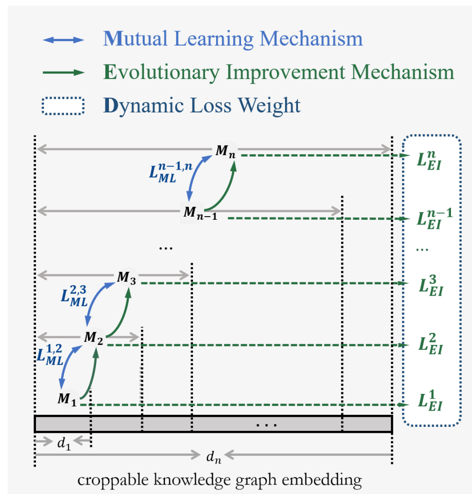

Figure 2: Overview of MED.

MED is based on knowledge distillation Hinton et al. (2015); Tang et al. (2019); Devlin et al. (2019) technique that the student learns by fitting the hard (ground-truth) label and the soft label from the teacher simultaneously. In MED, we first propose a *mutual learning mechanism* that makes low-dimensional sub-models learn from high-dimensional sub-models to achieve better performance, and makes high-dimensional sub-models also learn from low-dimensional sub-models to retain the abilities that low-dimensional sub-models already have. Then, we propose an *evolutionary improvement mechanism* to enable high-dimensional sub-models to master the knowledge that the low-dimensional sub-models can not learn well. Finally, we train MED with *dynamic loss weight* to adaptively balance multiple optimization objectives of sub-models.

4.1 Mutual Learning Mechanism

We treat each sub-model M_i as the student of its higher-dimensional neighbor sub-model M_{i+1} to achieve better performance, since high-dimensional KGEs usually have more expressive power than low-dimensional ones due to more parameters Sachan (2020); Zhu et al. (2022). We also treat sub-model M_i as the student of its lower-dimensional neighbor sub-model M_{i-1}, so the higher-dimensional sub-model can review what the lower-dimensional sub-model has learned and retain the low-dimensional one's existing abilities. Thus, pairwise neighbor sub-models serve as both teachers and students, learning from each other. The mutual learning loss between each pair of neighbor sub-models is

$$L_{ML}^{i-1,i} = \sum_{(h,r,t)\in\mathcal{T}\cup\mathcal{T}^-} d_\delta\left(s_{(h,r,t)}^{i-1}, s_{(h,r,t)}^{i}\right), 1 < i \leqslant n, \tag{2}$$

where $s_{(h,r,t)}^{i}$ is the score of triple (h, r, t) output by sub-model M_i and reflects the possibility that this triplet exists, $\mathcal{T}^- = \mathcal{E} \times \mathcal{R} \times \mathcal{E} \setminus \mathcal{T}$ is the negative triple set, n is the number of sub-models, and d_δ is Huber loss Huber & Peter (1964) with $\delta = 1$ commonly used in knowledge distillation for KGE Zhu et al. (2022). MED makes each sub-model only learn from its neighbor sub-models. The advantage is that this not only reduces the computational complexity of training but also makes every pair of teacher and student models have a relatively small dimension gap, which is important and effective because the large gap of dimensions between teacher and student will destroy the distillation effect Mirzadeh et al. (2020); Zhu et al. (2022).

4.2 Evolutionary Improvement Mechanism

The hard (ground-truth) label is the other important supervision signal during training in knowledge distillation Hinton et al. (2015). High-dimensional sub-models need to master triples that low-dimensional sub-models can not learn well, that is, high-dimensional sub-models need to correctly predict those positive (negative) triples that are wrongly predicted to be negative (positive) by low-dimensional sub-models. In MED, for a given triple (h, r, t), the optimization weight in sub-model M_i for it depends on the triple score output by the previous sub-model M_{i-1}.

For a positive triple, the optimization weight of the model M_i for it is negatively correlated with its score by the model M_{i-1}. Specifically, the higher its score from the model M_{i-1} (meaning that M_{i-1} has been able to correctly judge it as a positive sample), the lower the optimization weight of the model M_i for it, and the lower its score from the model M_{i-1} (meaning that M_{i-1} wrongly judges it as a negative sample), the higher the optimization weight of the model M_i for it because M_{i-1} cannot predict this triple well. The optimization weight of M_i for the positive triple is

$$pos_{h,r,t}^{i} = \frac{\exp w_1 / s_{(h,r,t)}^{i-1}}{\sum_{(h,r,t)\in T_{batch}} \exp w_1 / s_{(h,r,t)}^{i-1}} \; \texttt{if}\; 1 < i \leqslant n\,; \quad \frac{1}{|T_{batch}|} \; \texttt{if}\; i = 1, \tag{3}$$

where $s_{(h,r,t)}^{i-1}$ is the score for triple (h, r, t) output by the sub-model M_{i-1}, T_{batch} is the set of positive triples within a batch, and w_1 is a learnable scaling parameter. Conversely, for a negative triple, the optimization weight of the model M_i for it is positively correlated with its score by the model M_{i-1} Sun et al. (2019b), and the optimization weight of M_i for the negative triple is

$$neg_{h,r,t}^{i} = \frac{\exp w_2 \cdot s_{(h,r,t)}^{i-1}}{\sum_{(h,r,t)\in T_{batch}^-} \exp w_2 \cdot s_{(h,r,t)}^{i-1}} \; \texttt{if}\; 1 < i \leqslant n\,; \quad \frac{1}{|T_{batch}^-|} \; \texttt{if}\; i = 1, \tag{4}$$

where T_{batch}^- is the set of negative triples within a batch, and w_2 is a learnable scaling parameter.

Therefore, the evolutionary improvement loss of the sub-model M_i is

$$L_{EI}^{i} = -\sum_{(h,r,t)\in\mathcal{T}\cup\mathcal{T}^-} pos_{h,r,t}^{i} \cdot y \log \sigma(s_{(h,r,t)}^{i}) + neg_{h,r,t}^{i} \cdot (1-y) \log(1 - \sigma(s_{(h,r,t)}^{i})), \tag{5}$$

where σ is the Sigmoid activation function, y is the ground-truth label of the triple (h, r, t), and it is 1 for positive triples and 0 for negative ones. In each sub-model, different hard (ground-truth) label loss weights are set for different triples, and the high-dimensional sub-model will pay more attention to learn the triple that the low-dimensional sub-model can not learn well.

4.3 Dynamic Loss Weight

Since MED involves the optimization of multiple sub-models, we set dynamic loss weights during training. Initially, low-dimensional sub-models prioritize learning from high-dimensional sub-models to improve performance. This means low-dimensional sub-models rely more on soft label information, so for low-dimensional sub-models, evolutionary improvement loss should account for less than mutual learning loss. Conversely, high-dimensional sub-models should focus more on capturing knowledge that low-dimensional models lack, while mitigating the impact of low-quality outputs from low-dimensional models to maintain their good performance, that is, high-dimensional sub-models rely more on hard label information. So for high-dimensional sub-models, evolutionary improvement loss should account for more than mutual learning loss. For a teacher-student pair, their mutual learning loss acts on both teacher and student models simultaneously, so the effect of mutual learning loss for them is theoretically the same. We set different evolutionary improvement loss weights for different sub-models, and the final training loss function of MED is

$$L = \sum_{i=2}^{n} L_{ML}^{i-1,i} + \sum_{i=1}^{n} \exp(\frac{w_3 \cdot d_i}{d_n}) \cdot L_{EI}^{i}, \tag{6}$$

where w_3 is a learnable scaling parameter, and d_i is the dimension of the ith sub-model.

5 EXPERIMENT

We evaluate MED on typical KGE and GLUE benchmarks and particularly answer the following research questions: (**RQ1**) Is it capable for MED to train a croppable KGE at once that multiple sub-models of different dimensions can be cropped from it and all achieve promising performance? (**RQ2**) Can MED finally achieve parameter-efficient KGE models? (**RQ3**) Does MED work in real-world applications? (**RQ4**) Can MED be extended to other neural networks besides KGE?

5.1 EXPERIMENT SETTING

5.1.1 DATASET AND KGE METHODS

MED is universal and can be applied to any KGE method with a triple score function, we select three commonly used KGE methods as examples: TransE Bordes et al. (2013), SimplE Kazemi & Poole (2018), RotatE Sun et al. (2019b) and PairRE Chao et al. (2021), the triple score functions are described in Table 1.

We conduct comparison experiments on two common KG completion benchmark datasets WN18RR Toutanova et al. (2015) and FB15K237 Dettmers et al. (2018) and two more larger-scale KGs CoDEx-L Safavi & Koutra (2020) and YAGO3-10 Mahdisoltani et al. (2015). Besides, we apply our MED on a real-world large-scale e-commerce social knowledge graph (SKG) involving more than 50 million triples of social records by about 7 million users in the Taobao platform in real application scenarios. Table 2 shows the statistics of the datasets.

Table 2: Statistics of datasets.

Dataset	#Ent.	#Rel.	#Train	#Valid	#Test
WN18RR	40,943	11	86,835	3,034	3,134
FB15K237	14,541	237	272,115	17,535	20,466
CoDEx-L	77,951	69	551,193	30,622	30,622
YAGO3-10	123,143	37	1,079,040	4,978	4,982
SKG	6,974,959	15	50,775,620	-	-

5.1.2 EVALUATION METRIC

For the link prediction task, we adopt standard metrics MRR and Hit@k $(k = 1, 3, 10)$ in the filtered setting Bordes et al. (2013). For a test triple (h, r, t), we construct candidate triples by replacing h with all entities and keeping the replaced triples not in training, validation, and test set. Then we calculate the triple score rank of (h, r, t) among all candidate triples as its head prediction rank $rank_t$. Similarly, we get its tail prediction rank $rank_t$. We average $rank_h$ and $rank_t$ as (h, r, t)'s final rank. MRR is the mean reciprocal rank of all test triples, and Hit@k is the percentage of test triples with rank $\leq k$. We use *Effi* Chen et al. (2023), that is *MRR/#P* (*#P* is the number of parameters), to quantify the parameter efficiency of models. We use f1-score and accuracy for user labeling task, and normalized discounted cumulative gain ndcg@$k(k = 5, 10)$ for product recommendation task.

5.1.3 IMPLEMENTATION

For the link prediction task, we set $d_n = 640$ for the highest-dimensional sub-model M_n and $d_1 = 10$ for the lowest-dimensional sub-model M_1. We set $n = 64$ and the dimension gap 10 for every pair of neighbor sub-models. There are a total of 64 available sub-models of different dimensions from 10 to 640 in our croppable KGE model. The dimension of sub-model $M_i(i = 1, 2..., 64)$ is $10 \times i$. For the user labeling and product recommendation task, we set $n = 3$ and train the croppable KGE containing 3 sub-models: M_1 with $d_1 = 10$ for mobile phone (MB) terminals that are limited by storage and computing resources, M_2 with $d_2 = 100$ for the personal computer (PC), and M_3 with $d_3 = 500$ for the platform's servers. We initialize the learnable scaling parameters w_i, w_2 and w_3 in equation 3, equation 4 and equation 6 to 1. We implement MED by extending OpenKE Han et al. (2018), an open-source KGE framework based on PyTorch. We set the batch size to 1024 and the maximum training epoch to 3000 with early stopping. For each positive triple, we generate 64 negative triples by randomly replacing its head or tail entity with another entity. We use Adam Kingma & Ba (2015) optimizer with a linear decay learning rate scheduler and perform a search on the initial learning rate in $\{0.0001, 0.0005, 0.001, 0.01\}$. We train all sub-models simultaneously by optimizing the uniformly sampled sub-models from the full Croppable model in each step.

5.1.4 BASELINES

For each required dimension d_r, we extract the first d_r dimensions from our croppable KGE as the target model and compare it to the KGE models obtained by 8 baselines of the following 3 types:

- Directly training the target KGE model of requirement dimension d_r, referred to as **1) DT**. The directly trained highest-dimensional KGE model ($d_r = d_n$) is marked as M^{DT}_{max}.
- Extracting the first d_r dimensions from M^{DT}_{max} as the target model, referred to as **2) Ext**. Besides, we update M^{DT}_{max} by assessing the importance of each one of 640 dimensions and arranging them in descending order before extracting as Molchanov et al. (2017); Voita et al. (2019): **3) Ext-L**, the importance for each dimension of M^{DT}_{max} is the variation of KGE loss on validation set after removing it; and **4) Ext-V**, the importance for each dimension is the average absolute of its parameter weights of all entities and all relations.
- Distilling the target KGE by KD methods: **5) BKD** Hinton et al. (2015) is the most basic one by minimizing the KL divergence of the output distributions of teacher and student; **6) TA** Mirzadeh et al. (2020) uses a medium-size teaching assistant (TA) model as a bridge for size gap, where TA model has the same dimension as the directly trained one whose MRR is closest to the average MRR of teacher and student. We also compare with two KD methods proposed for KGE, which have similar configurations to ours, i.e. compressing high-dimensional teacher into low-dimensional student: **7) DualDE** Zhu et al. (2022) considers the mutual influences between teacher and student and optimizes them simultaneously; **8) IterDE** Liu et al. (2023) enables the KGE model to alternately act as student and teacher so that knowledge can be transferred smoothly between high-dimensional teacher and low-dimensional student. In these baselines, M^{DT}_{max} is the teacher, and other settings including hyperparameters are the same as their original papers.

5.2 PERFORMANCE COMPARISON

We report the link prediction results of some representative dimensions in Table 3, more results of other dimensions and metrics are in Appendix A and the ablation studies are in Appendix B.

MED outperforms baselines in almost all settings, especially for the extremely low dimensions. On WN18RR with d=10, MED achieves an improvement of **14.9%** and **15.1%** on TransE, **8.4%** and **6.6%** on RotatE, **29.4%** and **10.6%** on PairRE compared with the best MRR and Hit@10 of baselines. We can observe a similar phenomenon on FB15K237. This benefits from the rich knowledge sources of low-dimensional models in MED: For sub-model M_i, M_{i+1} is the teacher directly next to it, while M_{i+2} can also indirectly affect M_i by directly affecting M_{i+1}. Theoretically, all higher-dimensional sub-models can finally transfer their knowledge to low-dimensional sub-models through stepwise propagation. Although such stepwise propagation may have negative effects on high-dimensional models by bringing low-quality knowledge from low-dimensional sub-models, the evolutionary improvement mechanism in MED weakens the damage and makes high-dimensional ones still achieve competitive performance than directly trained KGEs as in Fig. 3. We also find that Ext-based methods perform extremely unstable: Ext, Ext-L, and Ext-V work worse than DT except on WN18RR with TransE, indicating that only considering the importance of each dimension is not enough to guarantee the performance of all sub-models. More results and ablation studies are in Appendix A and Appendix B.

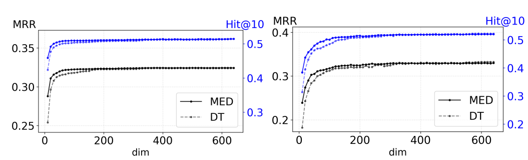

Figure 3: Results of different dimensions for PairRE on WN18RR (left) and FB15K237 (right).

Table 3: MRR and Hit@10 (H10) of some dimensions on WN18RR (WN) and FB15K237 (FB).

		WN18RR								FB15K237							
		10d		40d		160d		640d		10d		40d		160d		640d	
KGE	*Method*	*MRR*	*H10*	*MRR*	*H10*	*MRR*	*H10*	*MRR*	*H10*	*MRR*	*H10*	*MRR*	*H10*	*MRR*	*H10*	*MRR*	*H10*
TransE	DT	0.121	0.287	0.214	0.496	0.233	0.531	0.237	0.537	0.150	0.235	0.299	0.477	0.315	0.499	0.322	**0.508**
	Ext	0.125	0.298	0.199	0.468	0.225	0.515	0.237	0.537	0.115	0.211	0.236	0.392	0.286	0.462	0.322	0.508
	Ext-L	0.139	0.315	0.224	0.497	0.236	**0.534**	0.237	0.537	0.109	0.194	0.232	0.381	0.285	0.462	0.322	0.508
	Ext-V	0.139	0.309	0.222	0.494	0.236	0.532	0.237	0.537	0.139	0.256	0.237	0.396	0.293	0.466	0.322	0.508
	BKD	0.141	0.323	0.226	0.513	0.233	0.531	-	-	0.176	0.293	0.303	0.480	0.315	0.501	-	-
	TA	0.144	0.335	0.226	0.512	0.234	0.533	-	-	0.175	0.246	0.303	0.484	0.319	0.504	-	-
	DualDE	0.148	0.337	0.225	0.514	0.235	0.533	-	-	0.179	0.301	0.306	0.483	0.319	0.505	-	-
	IterDE	0.143	0.332	0.224	0.511	0.236	0.531	-	-	0.176	0.285	0.307	0.482	0.317	0.505	-	-
	MED	**0.170**	**0.388**	**0.232**	**0.518**	**0.236**	0.529	**0.237**	**0.537**	**0.196**	**0.341**	**0.308**	**0.486**	**0.320**	**0.505**	**0.322**	0.507
SimplE	DT	0.061	0.126	0.316	0.389	0.409	0.459	0.421	0.481	0.097	0.179	0.236	0.390	0.285	0.458	**0.295**	**0.472**
	Ext	0.004	0.007	0.160	0.249	0.357	0.401	0.421	0.481	0.037	0.068	0.090	0.144	0.229	0.372	0.295	0.472
	Ext-L	0.005	0.006	0.169	0.244	0.398	0.454	0.421	0.481	0.045	0.059	0.083	0.146	0.196	0.316	0.295	0.472
	Ext-V	0.004	0.006	0.246	0.317	0.398	0.461	0.421	0.481	0.049	0.069	0.105	0.149	0.224	0.369	0.295	0.472
	BKD	0.075	0.156	0.343	0.399	0.414	0.468	-	-	0.113	0.204	0.244	0.412	0.287	0.463	-	-
	TA	0.089	0.189	0.368	0.418	0.415	0.472	-	-	0.124	0.221	0.254	0.416	0.290	0.465	-	-
	DualDE	0.083	0.175	**0.386**	0.423	**0.419**	0.475	-	-	0.120	0.213	0.258	**0.429**	0.293	0.466	-	-
	IterDE	0.077	0.162	0.375	0.419	0.416	0.469	-	-	0.120	0.215	0.257	0.427	**0.293**	0.465	-	-
	MED	**0.111**	**0.224**	0.385	**0.431**	0.418	**0.477**	**0.421**	**0.482**	**0.143**	**0.267**	**0.261**	0.427	0.291	**0.466**	0.294	0.470
RotatE	DT	0.172	0.418	0.456	0.556	0.471	0.567	0.476	0.575	0.254	0.424	0.312	0.495	0.322	0.506	**0.325**	**0.515**
	Ext	0.299	0.378	0.437	0.516	0.467	0.549	0.476	**0.575**	0.138	0.245	0.251	0.410	0.291	0.465	0.325	0.515
	Ext-L	0.206	0.277	0.399	0.487	0.445	0.541	0.476	0.575	0.135	0.243	0.221	0.365	0.280	0.453	0.325	0.515
	Ext-V	0.261	0.377	0.337	0.471	0.416	0.532	0.476	0.575	0.160	0.281	0.238	0.393	0.288	0.458	0.325	0.515
	BKD	0.175	0.434	0.457	0.556	0.472	0.570	-	-	0.277	0.442	0.314	0.503	0.322	0.510	-	-
	TA	0.177	0.438	0.459	0.558	0.473	0.572	-	-	0.280	0.447	0.313	0.501	0.323	0.510	-	-
	DualDE	0.179	0.440	0.462	0.559	**0.473**	0.573	-	-	0.282	0.449	0.315	0.502	0.322	**0.512**	-	-
	IterDE	0.176	0.436	0.459	0.560	0.471	0.569	-	-	0.276	0.445	0.317	0.504	0.323	0.512	-	-
	MED	**0.324**	**0.469**	**0.466**	**0.561**	0.471	**0.574**	**0.476**	0.574	**0.288**	**0.459**	**0.318**	**0.504**	**0.323**	0.510	0.324	0.514
PairRE	DT	0.220	0.321	0.415	0.472	0.449	0.534	**0.453**	**0.544**	0.182	0.314	0.284	0.452	0.319	0.505	**0.332**	**0.522**
	Ext	0.152	0.209	0.334	0.463	0.419	0.526	0.453	0.544	0.148	0.222	0.217	0.353	0.294	0.469	0.332	0.522
	Ext-L	0.162	0.220	0.363	0.442	0.437	0.523	0.453	0.544	0.150	0.249	0.219	0.333	0.309	0.489	0.332	0.522
	Ext-V	0.172	0.260	0.389	0.456	0.441	0.529	0.453	0.544	0.176	0.277	0.229	0.374	0.311	0.490	0.332	0.522
	BKD	0.228	0.336	0.421	0.483	0.451	0.536	-	-	0.198	0.332	0.288	0.453	0.321	0.508	-	-
	TA	0.245	0.340	0.426	0.487	0.452	0.537	-	-	0.208	0.346	0.292	0.455	0.323	0.509	-	-
	DualDE	0.242	0.336	0.428	0.495	**0.453**	0.540	-	-	0.207	0.342	0.293	0.456	**0.326**	**0.512**	-	-
	IterDE	0.235	0.336	0.426	0.495	0.450	0.538	-	-	0.205	0.340	0.293	0.462	0.324	0.508	-	-
	MED	**0.317**	**0.376**	**0.433**	**0.502**	0.451	**0.541**	0.451	0.542	**0.239**	**0.384**	**0.303**	**0.466**	0.324	0.510	0.330	0.520

5.3 PARAMETER EFFICIENCY OF MED

In Table 4, we compare our sub-models of suitable low dimensions to parameter-efficient KGEs especially proposed for large-scale KGs including NodePiece Galkin et al. (2022) and EARL Chen et al. (2023). In the case that the number of model parameters is roughly equivalent, the performance of the sub-models of MED exceeds that of the specialized parameter-efficient KGE methods. This demonstrates sub-models of our method are parameter efficient. More importantly, it can provide parameter-efficient models of different size for applications.

Table 4: Link prediction results on WN18RR, FB15K237, CoDEx-L and YAGO3-10.

	FB15k-237					WN18RR					CoDEx-L					YAGO3-10				
	Dim	*#P(M)*	*MRR*	*Hit@10*	*Effi*	*Dim*	*#P(M)*	*MRR*	*Hit@10*	*Effi*	*Dim*	*#P(M)*	*MRR*	*Hit@10*	*Effi*	*Dim*	*#P(M)*	*MRR*	*Hit@10*	*Effi*
RotatE	1000	29.3	0.336	0.532	0.011	500	40.6	0.508	0.612	0.013	500	78	0.258	0.387	0.003	500	123.2	0.495	0.670	0.004
RotatE	100	2.9	0.296	0.473	0.102	50	4.1	0.411	0.429	0.100	25	3.8	0.196	0.322	0.052	20	4.8	0.121	0.262	0.025
+ NodePiece	100	3.2	0.256	0.420	0.080	100	4.4	0.403	0.515	0.092	100	3.6	0.190	0.313	0.053	100	4.1	0.247	0.488	0.060
+ EARL	150	1.8	0.310	0.501	0.172	200	3.8	0.440	0.527	0.116	100	2.1	0.238	**0.390**	**0.113**	100	3	0.302	0.498	**0.101**
+ MED	40	1.2	**0.318**	**0.504**	**0.265**	40	3.2	**0.466**	**0.561**	**0.146**	20	3.1	**0.243**	0.385	0.078	20	4.9	**0.313**	**0.528**	0.064

5.4 MED IN REAL APPLICATIONS

Table 5: Results on SKG.

		User Labeling		Product Recommendation			
		server (500d)		PC terminal (100d)		MP terminal (10d)	
Method	*train time*	*acc.*	*f1*	*ndcg@5*	*ndcg@10*	*ndcg@5*	*ndcg@10*
DT	103h	0.889	0.874	0.411	0.441	0.344	0.361
PCA	-	-	-	0.417	0.447	0.392	0.418
DualDE	195h	-	-	0.423	0.456	0.404	0.433
MED	53h	**0.893**	**0.879**	**0.431**	**0.465**	**0.422**	**0.451**

We apply the trained croppable KGE with TransE on SKG to three real applications: the user labeling task on servers and the product recommendation task on PCs and mobile phones. Table 5 shows that our croppable user embeddings substantially exceed all baselines including directly trained (DT), the best baseline DualDE, and a common dimension reduction method in industry principal components analysis (PCA) on M_{max}^{DT}. Notably, the excellent performance on the mobile phone task (which can only carry embeddings with a maximum dimension of 10 limited by storage and computing resources) demonstrates the enormous practical value of our approach. More application details are in Appendix C.

5.5 EXTEND MED TO NEURAL NETWORKS

To verify the extensibility of our method to other neural networks, we take the language model BERT Devlin et al. (2019) as an example. We uniformly adopt distillation methods implemented based on Hugging Face Transformers Wolf et al. (2020) as baselines. Following previous works Sun et al. (2019a); Tang et al. (2019); Jung et al. (2023); Zhou et al. (2022a), we distill at the fine-tuning stage. More experimental details are in Appendix D.

Table 6: Results on the dev set of GLUE. The results of knowledge distillation methods for BERT_4 and BERT_6 are reported by Jung et al. (2023); Zhou et al. (2022a) and the †results reported by us.

Method	*#P(M)*	*Speedup*	MNLI-m *acc.*	MNLI-mm *acc.*	MRPC *f1/acc.*	QNLI *acc.*	QQP *f1/acc.*	RTE *acc.*	STS-2 *acc.*	STS-B *pear./spear.*
$\text{BERT}^{\dagger}_{Base}$	110	1.0×	84.4	85.3	88.6/84.1	89.7	89.6/91.1	67.5	92.5	88.8/88.5
BERT_6-BKD	66	2.0×	82.2	82.9	86.2/80.8	88.5	88.0/91.0	65.4	90.9	88.2/87.8
BERT_6-PKD	66	2.0×	82.3	82.6	86.4/81.0	88.6	87.9/91.0	63.9	90.8	88.5/88.1
BERT_6-MiniLM	66	2.0×	82.2	82.6	84.6/78.1	**89.5**	87.2/90.5	61.5	90.2	87.8/87.5
BERT_6-RKD	66	2.0×	82.4	82.9	86.9/81.8	88.9	88.1/**91.2**	65.2	91.0	88.4/88.1
BERT_6-FSD	66	2.0×	82.4	83.0	87.1/82.2	89.0	88.1/**91.2**	66.6	91.0	**88.7/88.3**
BERT_4-BKD	55	2.9×	80.5	80.9	87.2/83.1	87.5	86.6/90.4	65.2	90.2	84.5/84.2
BERT_4-PKD	55	2.9×	80.9	81.3	87.0/82.9	87.7	86.8/90.5	66.1	90.5	84.3/84.0
BERT_4-MetaDistil	55	2.9×	82.4	82.7	**88.4/84.2**	88.6	87.8/90.8	**67.8**	91.8	86.3/86.0
BERT-HAT†	54	2.0×	70.8	71.6	81.2/74.8	65.3	76.1/80.4	52.7	84.3	79.6/80.1
BERT-MED	54	2.0×	**82.7**	**83.3**	88.0/84.0	86.8	**89.1**/90.7	67.2	**91.9**	87.6/87.2
BERT-HAT†	17.5	4.7×	63.6	64.2	68.4/78.4	61.1	69.0/79.7	47.2	82.9	74.1/75.8
BERT-MED	17.5	4.7×	81.2	82.4	86.1/82.0	86.4	83.8/86.2	64.6	88.2	86.1/86.4
BERT-HAT†	6.36	5.2×	59.9	60.0	66.5/77.3	60.1	66.5/77.1	46.2	81.7	71.9/70.4
BERT-MED	6.36	5.2×	72.6	73.7	84.1/78.1	86.0	79.6/82.7	61.7	86.9	82.8/81.6

Table 6 shows the results on the development set of GLUE Wang et al. (2019). We compare MED with other KD models under similar speedup or a comparable number of parameters. MED achieves competitive performance on most tasks compared to BERT-specialized KD methods. In addition, when compared to HAT Wang et al. (2020a), which shares the most similar model architecture to ours, sub-models of MED outperform HAT across three different parameter quantities. Specifically, sub-models with 54M, 17.5M, and 6.36M parameters achieve average 16.3%, 21.7% and 19.7% improvements respectively.

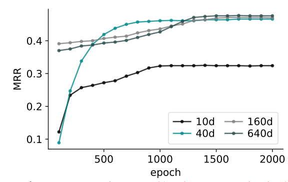

Figure 4: Sub-models' MRR during training on WN18RR with RotatE.

5.6 Analysis of MED

5.6.1 Training efficiency

We report the training time of obtaining 64 models of all sizes (d=10, 20, ..., 640) by different methods in Table 7. Figure 4 showing how the MRR of different sub-models changes during training. For DT, the training time cost is the sum of the time of directly training 64 KGE models of all sizes in turn. For the Ext-based baselines, the training time cost is the same and is equal to the time of training a d_n-dimensional KGE model since the time of arranging dimensions is very short and negligible. For the KD-based baselines, the training time cost is the sum of the time of training the d_n-dimensional teacher model and distilling 63 student models (d=10, 20, ..., 630) in turn. All training is performed on a single NVIDIA Tesla A100 40GB GPU for fair comparison. For TA, DualDE and IterDE on FB15K237, we don't train student models of all 63 sizes, which is estimated to take more than 400 hours on each KGE method. Compared with directly trained (DT) models of all sizes in turn, MED accelerates by up to 10× for 4 KGE methods. Although Ext-based baselines spend the shortest training time, they perform particularly poorly and lack practical value. Except for BKD, KD-based methods need to optimize both the student model and larger teacher model, which greatly increases the training parameters and time cost.

Table 7: Training time (hours).

		TransE		**SimplE**		**RotatE**		**PairRE**	
WN	DT	74.0	(9.49×)	68.0	(12.14×)	141.0	(11.10×)	67.4	(10.06×)
	Ext-based	1.5	(0.19×)	1.3	(0.23×)	2.5	(0.20×)	1.6	(0.24×)
	BKD	91.5	(11.73×)	72.0	(12.86×)	163.0	(12.83×)	87.5	(13.06×)
	TA	172.0	(22.05×)	142.0	(25.36×)	272.0	(21.42×)	166.0	(24.78×)
	DualDE	151.0	(19.36×)	133.0	(23.75×)	240.0	(18.90×)	133.0	(19.85×)
	IterDE	140.9	(18.06×)	118.0	(21.07×)	216.0	(17.01×)	124.0	(18.51×)
	MED	7.8	(1.00×)	5.6	(1.00×)	12.7	(1.00×)	6.7	(1.00×)
FB	DT	218.0	(10.23×)	179.0	(10.65×)	381.0	(10.73×)	179.0	(9.37×)
	Ext-based	4.7	(0.22×)	5.1	(0.30×)	9.5	(0.27×)	3.7	(0.19×)
	BKD	248.0	(11.64×)	227.0	(13.51×)	443.0	(12.48×)	231.0	(12.09×)
	MED	21.3	(1.00×)	16.8	(1.00×)	35.5	(1.00×)	19.1	(1.00×)

5.6.2 Effect of the number of sub-models

We set the number of different sub-models, i.e. n= 64, 16, 4 on WN18RR with RotatE. And Table 8 shows that when the number of sub-models is reduced, the performance of high-dimensional (d=160 and 640)

Table 8: Results of different n.

		10d		**40d**		**160d**		**640d**	
n	*train time*	*MRR*	*H10*	*MRR*	*H10*	*MRR*	*H10*	*MRR*	*H10*
64	12.7h	0.324	0.469	0.466	0.561	0.471	0.574	0.476	0.574
16	6.2h	0.322	0.467	0.465	0.561	0.473	0.575	0.477	0.576
4	3.3h	0.319	0.463	0.463	0.561	0.475	0.577	0.480	0.578

models improves, while the performance of low-dimensional (d=10 and 40) models decreases (still exceeds the best result of baselines in Table 3 that MRR=0.299 of Ext with d=10, MRR=0.462 of DualDE with d=40). The training efficiency is almost linearly related to the number of models.

5.6.3 Whether high-dimensional sub-models cover the capabilities of low-dimensional ones

If a high-dimensional model retains the ability of lower-dimensional models, it should correctly predict all triples that the lower-dimensional model can predict. We count the percentage of triples in test set that meet the condition that if the smallest sub-model that can correctly predict a given triple is M_i, all higher-dimensional sub-models (M_{i+1}, M_{i+2}, ..., M_n) also correctly predict it, and denote the result as the ability retention ratio (ARR). We use Hit@10 to judge whether a triple is correctly predicted, that is, M_i correctly predicts a triple if M_i scores this triple in the top 10 among all candidate triples.

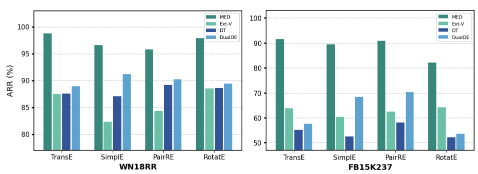

Figure 5: The ability retention ratio (ARR).

From Fig. 5, ARR of MED is always much higher than baselines, especially on FB15K237, indicating that high-dimensional sub-models in MED successfully cover the power of low-dimensional ones, contributed by the mutual learning mechanism that helps high-dimensional sub-models review what low-dimensional sub-models have learned. Based on this advantage of MED, we can provide a simple way to judge how easy or difficult a triple is for KGE methods to learn: the triple that low-dimensional sub-models can correctly predict may be easy since high-dimensional models can also predict it, while triples that can only be predicted by high-dimensional sub-models are difficult.

5.6.4 Visual analysis of embedding

We select four primary entity categories (‘organization’, ‘sports’, ‘location’, and ‘music’) that contain more than 300 entities in FB15K237, and randomly select 250 entities for each. We cluster these entities’ embeddings of 3 different dimensions (d=10, 100, 600) by the t-SNE algorithm, and the clustering results are visualized in Fig. 6. Under the same dimension, the clustering result of MED is always the best, followed by DualDE, while the result of Ext-V is generally poor, which is consistent with the conclusion in Section 5.2. We also find some special phenomenons for MED when dimension increases: 1) the nodes of the ‘sports’ gradually become two clusters meaning MED learns more fine-grained category information as dimension increases. and 2) the relative distribution among different categories hardly changes and shows a trend of “inheritance” and “improvement”. This further proves MED achieves our expectation that high-dimensional sub-models retain the ability of low-dimensional sub-models, and can learn more knowledge than low-dimensional sub-models.

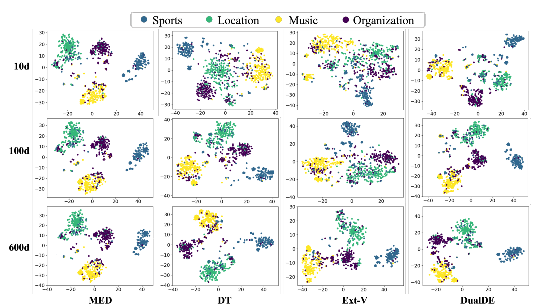

Figure 6: Clustering on FB15K237 with RotatE.

6 Conclusion

In this work, we propose a novel KGE training framework, MED, that trains a croppable KGE at once, and then sub-models of various required dimensions can be cropped out from it and used directly without additional training. In MED, we propose the mutual learning mechanism to improve low-dimensional sub-models performance and make the high-dimensional sub-models retain the ability of the low-dimensional ones, the evolutionary improvement mechanism to motivate high-dimensional sub-models to master more knowledge that low-dimensional ones cannot, and the dynamic loss weight to adaptively balance multiple losses. The experimental results show the effectiveness and high efficiency of our method, where all sub-models achieve promising performance, especially the performance of low-dimensional sub-models is greatly improved. In future work, we will further explore the more fine-grained information encoding ability of each sub-model.

REFERENCES

Haoli Bai, Wei Zhang, Lu Hou, Lifeng Shang, Jin Jin, Xin Jiang, Qun Liu, Michael R. Lyu, and Irwin King. Binarybert: Pushing the limit of BERT quantization. In *ACL/IJCNLP (1)*, pp. 4334–4348. Association for Computational Linguistics, 2021.

Antoine Bordes, Nicolas Usunier, Alberto García-Durán, Jason Weston, and Oksana Yakhnenko. Translating embeddings for modeling multi-relational data. In *NIPS*, pp. 2787–2795, 2013.

Linlin Chao, Jianshan He, Taifeng Wang, and Wei Chu. Pairre: Knowledge graph embeddings via paired relation vectors. In *ACL/IJCNLP (1)*, pp. 4360–4369. Association for Computational Linguistics, 2021.

Mingyang Chen, Wen Zhang, Zhen Yao, Yushan Zhu, Yang Gao, Jeff Z. Pan, and Huajun Chen. Entity-agnostic representation learning for parameter-efficient knowledge graph embedding. In *AAAI*, pp. 4182–4190. AAAI Press, 2023.

Alexis Conneau and Douwe Kiela. Senteval: An evaluation toolkit for universal sentence representations. In Nicoletta Calzolari, Khalid Choukri, Christopher Cieri, Thierry Declerck, Sara Goggi, Kôiti Hasida, Hitoshi Isahara, Bente Maegaard, Joseph Mariani, Hélène Mazo, Asunción Moreno, Jan Odijk, Stelios Piperidis, and Takenobu Tokunaga (eds.), *Proceedings of the Eleventh International Conference on Language Resources and Evaluation, LREC 2018, Miyazaki, Japan, May 7-12, 2018*. European Language Resources Association (ELRA), 2018. URL `http://www.lrec-conf.org/proceedings/lrec2018/summaries/757.html`.

Joachim Daiber, Max Jakob, Chris Hokamp, and Pablo N. Mendes. Improving efficiency and accuracy in multilingual entity extraction. In *I-SEMANTICS*, pp. 121–124. ACM, 2013.

Tim Dettmers, Pasquale Minervini, Pontus Stenetorp, and Sebastian Riedel. Convolutional 2d knowledge graph embeddings. In *AAAI*, pp. 1811–1818. AAAI Press, 2018.

Jacob Devlin, Ming-Wei Chang, Kenton Lee, and Kristina Toutanova. BERT: pre-training of deep bidirectional transformers for language understanding. In *NAACL-HLT (1)*, pp. 4171–4186. Association for Computational Linguistics, 2019.

Dennis Diefenbach, Kamal Deep Singh, and Pierre Maret. Wdaqua-core1: A question answering service for RDF knowledge bases. In *WWW (Companion Volume)*, pp. 1087–1091. ACM, 2018.

William B. Dolan and Chris Brockett. Automatically constructing a corpus of sentential paraphrases. In *Proceedings of the Third International Workshop on Paraphrasing, IWP@IJCNLP 2005, Jeju Island, Korea, October 2005, 2005*. Asian Federation of Natural Language Processing, 2005. URL `https://aclanthology.org/I05-5002/`.

Cunhang Fan, Yujie Chen, Jun Xue, Yonghui Kong, Jianhua Tao, and Zhao Lv. Progressive distillation based on masked generation feature method for knowledge graph completion. In *AAAI*, pp. 8380–8388. AAAI Press, 2024.

Mikhail Galkin, Etienne G. Denis, Jiapeng Wu, and William L. Hamilton. Nodepiece: Compositional and parameter-efficient representations of large knowledge graphs. In *ICLR*. OpenReview.net, 2022.

Xu Han, Shulin Cao, Xin Lv, Yankai Lin, Zhiyuan Liu, Maosong Sun, and Juanzi Li. Openke: An open toolkit for knowledge embedding. In *EMNLP (Demonstration)*, pp. 139–144. Association for Computational Linguistics, 2018.

Xiangnan He, Lizi Liao, Hanwang Zhang, Liqiang Nie, Xia Hu, and Tat-Seng Chua. Neural collaborative filtering. In *WWW*, pp. 173–182. ACM, 2017.

Geoffrey E. Hinton, Oriol Vinyals, and Jeffrey Dean. Distilling the knowledge in a neural network. *CoRR*, abs/1503.02531, 2015.

Raphael Hoffmann, Congle Zhang, Xiao Ling, Luke S. Zettlemoyer, and Daniel S. Weld. Knowledge-based weak supervision for information extraction of overlapping relations. In *ACL*, pp. 541–550. The Association for Computer Linguistics, 2011.

Huber and J. Peter. Robust estimation of a location parameter. *The Annals of Mathematical Statistics*, 35(1):73–101, 1964.

Guoliang Ji, Shizhu He, Liheng Xu, Kang Liu, and Jun Zhao. Knowledge graph embedding via dynamic mapping matrix. In *ACL (1)*, pp. 687–696. The Association for Computer Linguistics, 2015.

Hee-Jun Jung, Doyeon Kim, Seung-Hoon Na, and Kangil Kim. Feature structure distillation with centered kernel alignment in BERT transferring. *Expert Syst. Appl.*, 234:120980, 2023. doi: 10.1016/J.ESWA.2023.120980. URL https://doi.org/10.1016/j.eswa.2023.120980.

Seyed Mehran Kazemi and David Poole. Simple embedding for link prediction in knowledge graphs. In *NeurIPS*, pp. 4289–4300, 2018.

Diederik P. Kingma and Jimmy Ba. Adam: A method for stochastic optimization. In *ICLR (Poster)*, 2015.

Yankai Lin, Zhiyuan Liu, Maosong Sun, Yang Liu, and Xuan Zhu. Learning entity and relation embeddings for knowledge graph completion. In *AAAI*, pp. 2181–2187. AAAI Press, 2015.

Jiajun Liu, Peng Wang, Ziyu Shang, and Chenxiao Wu. Iterde: An iterative knowledge distillation framework for knowledge graph embeddings. In *AAAI*, pp. 4488–4496. AAAI Press, 2023.

Jiajun Liu, Wenjun Ke, Peng Wang, Ziyu Shang, Jinhua Gao, Guozheng Li, Ke Ji, and Yanhe Liu. Towards continual knowledge graph embedding via incremental distillation. In *AAAI*, pp. 8759–8768. AAAI Press, 2024.

Farzaneh Mahdisoltani, Joanna Biega, and Fabian M. Suchanek. YAGO3: A knowledge base from multilingual wikipedias. In *CIDR*. www.cidrdb.org, 2015.

Seyed-Iman Mirzadeh, Mehrdad Farajtabar, Ang Li, Nir Levine, Akihiro Matsukawa, and Hassan Ghasemzadeh. Improved knowledge distillation via teacher assistant. In *AAAI*, pp. 5191–5198. AAAI Press, 2020.

Pavlo Molchanov, Stephen Tyree, Tero Karras, Timo Aila, and Jan Kautz. Pruning convolutional neural networks for resource efficient inference. In *ICLR (Poster)*. OpenReview.net, 2017.

Dai Quoc Nguyen, Tu Dinh Nguyen, Dat Quoc Nguyen, and Dinh Q. Phung. A novel embedding model for knowledge base completion based on convolutional neural network. In *NAACL-HLT (2)*, pp. 327–333. Association for Computational Linguistics, 2018.

Maximilian Nickel, Volker Tresp, and Hans-Peter Kriegel. A three-way model for collective learning on multi-relational data. In *ICML*, pp. 809–816. Omnipress, 2011.

Wonpyo Park, Dongju Kim, Yan Lu, and Minsu Cho. Relational knowledge distillation. In *CVPR*, pp. 3967–3976. Computer Vision Foundation / IEEE, 2019.

Pranav Rajpurkar, Jian Zhang, Konstantin Lopyrev, and Percy Liang. Squad: 100, 000+ questions for machine comprehension of text. In Jian Su, Xavier Carreras, and Kevin Duh (eds.), *Proceedings of the 2016 Conference on Empirical Methods in Natural Language Processing, EMNLP 2016, Austin, Texas, USA, November 1-4, 2016*, pp. 2383–2392. The Association for Computational Linguistics, 2016. doi: 10.18653/V1/D16-1264. URL https://doi.org/10.18653/v1/d16-1264.

Mrinmaya Sachan. Knowledge graph embedding compression. In *ACL*, pp. 2681–2691. Association for Computational Linguistics, 2020.

Tara Safavi and Danai Koutra. Codex: A comprehensive knowledge graph completion benchmark. In *EMNLP (1)*, pp. 8328–8350. Association for Computational Linguistics, 2020.

Michael Sejr Schlichtkrull, Thomas N. Kipf, Peter Bloem, Rianne van den Berg, Ivan Titov, and Max Welling. Modeling relational data with graph convolutional networks. In *ESWC*, volume 10843 of *Lecture Notes in Computer Science*, pp. 593–607. Springer, 2018.

Richard Socher, Alex Perelygin, Jean Wu, Jason Chuang, Christopher D. Manning, Andrew Y. Ng, and Christopher Potts. Recursive deep models for semantic compositionality over a sentiment treebank. In *Proceedings of the 2013 Conference on Empirical Methods in Natural Language Processing, EMNLP 2013, 18-21 October 2013, Grand Hyatt Seattle, Seattle, Washington, USA, A meeting of SIGDAT, a Special Interest Group of the ACL*, pp. 1631–1642. ACL, 2013. URL https://aclanthology.org/D13-1170/.

Pierre Stock, Angela Fan, Benjamin Graham, Edouard Grave, Rémi Gribonval, Hervé Jégou, and Armand Joulin. Training with quantization noise for extreme model compression. In *ICLR*. OpenReview.net, 2021.

Siqi Sun, Yu Cheng, Zhe Gan, and Jingjing Liu. Patient knowledge distillation for BERT model compression. In *EMNLP/IJCNLP (1)*, pp. 4322–4331. Association for Computational Linguistics, 2019a.

Zhiqing Sun, Zhi-Hong Deng, Jian-Yun Nie, and Jian Tang. Rotate: Knowledge graph embedding by relational rotation in complex space. In *ICLR (Poster)*. OpenReview.net, 2019b.

Raphael Tang, Yao Lu, Linqing Liu, Lili Mou, Olga Vechtomova, and Jimmy Lin. Distilling task-specific knowledge from BERT into simple neural networks. *CoRR*, abs/1903.12136, 2019.

Kristina Toutanova, Danqi Chen, Patrick Pantel, Hoifung Poon, Pallavi Choudhury, and Michael Gamon. Representing text for joint embedding of text and knowledge bases. In *EMNLP*, pp. 1499–1509. The Association for Computational Linguistics, 2015.

Théo Trouillon, Johannes Welbl, Sebastian Riedel, Éric Gaussier, and Guillaume Bouchard. Complex embeddings for simple link prediction. In *ICML*, volume 48 of *JMLR Workshop and Conference Proceedings*, pp. 2071–2080. JMLR.org, 2016.

Shikhar Vashishth, Soumya Sanyal, Vikram Nitin, and Partha P. Talukdar. Composition-based multi-relational graph convolutional networks. In *ICLR*. OpenReview.net, 2020.

Elena Voita, David Talbot, Fedor Moiseev, Rico Sennrich, and Ivan Titov. Analyzing multi-head self-attention: Specialized heads do the heavy lifting, the rest can be pruned. In *ACL (1)*, pp. 5797–5808. Association for Computational Linguistics, 2019.

Alex Wang, Amanpreet Singh, Julian Michael, Felix Hill, Omer Levy, and Samuel R. Bowman. GLUE: A multi-task benchmark and analysis platform for natural language understanding. In *7th International Conference on Learning Representations, ICLR 2019, New Orleans, LA, USA, May 6-9, 2019*. OpenReview.net, 2019. URL https://openreview.net/forum?id=rJ4km2R5t7.

Hanrui Wang, Zhanghao Wu, Zhijian Liu, Han Cai, Ligeng Zhu, Chuang Gan, and Song Han. HAT: hardware-aware transformers for efficient natural language processing. In *ACL*, pp. 7675–7688. Association for Computational Linguistics, 2020a.

Haoyu Wang, Yaqing Wang, Defu Lian, and Jing Gao. A lightweight knowledge graph embedding framework for efficient inference and storage. In *CIKM*, pp. 1909–1918. ACM, 2021a.

Kai Wang, Yu Liu, Qian Ma, and Quan Z. Sheng. Mulde: Multi-teacher knowledge distillation for low-dimensional knowledge graph embeddings. In *WWW*, pp. 1716–1726. ACM / IW3C2, 2021b.

Wenhui Wang, Furu Wei, Li Dong, Hangbo Bao, Nan Yang, and Ming Zhou. Minilm: Deep self-attention distillation for task-agnostic compression of pre-trained transformers. In Hugo Larochelle, Marc'Aurelio Ranzato, Raia Hadsell, Maria-Florina Balcan, and Hsuan-Tien Lin (eds.), *Advances in Neural Information Processing Systems 33: Annual Conference on Neural Information Processing Systems 2020, NeurIPS 2020, December 6-12, 2020, virtual*, 2020b. URL https://proceedings.neurips.cc/paper/2020/hash/3f5ee243547dee91fbd053c1c4a845aa-Abstract.html.

Zhen Wang, Jianwen Zhang, Jianlin Feng, and Zheng Chen. Knowledge graph embedding by translating on hyperplanes. In *AAAI*, pp. 1112–1119. AAAI Press, 2014.

Adina Williams, Nikita Nangia, and Samuel R. Bowman. A broad-coverage challenge corpus for sentence understanding through inference. In Marilyn A. Walker, Heng Ji, and Amanda Stent (eds.), *Proceedings of the 2018 Conference of the North American Chapter of the Association for Computational Linguistics: Human Language Technologies, NAACL-HLT 2018, New Orleans, Louisiana, USA, June 1-6, 2018, Volume 1 (Long Papers)*, pp. 1112–1122. Association for Computational Linguistics, 2018. doi: 10.18653/V1/N18-1101. URL `https://doi.org/10.18653/v1/n18-1101`.

Thomas Wolf, Lysandre Debut, Victor Sanh, Julien Chaumond, Clement Delangue, Anthony Moi, Pierric Cistac, Tim Rault, Rémi Louf, Morgan Funtowicz, Joe Davison, Sam Shleifer, Patrick von Platen, Clara Ma, Yacine Jernite, Julien Plu, Canwen Xu, Teven Le Scao, Sylvain Gugger, Mariama Drame, Quentin Lhoest, and Alexander M. Rush. Transformers: State-of-the-art natural language processing. In Qun Liu and David Schlangen (eds.), *Proceedings of the 2020 Conference on Empirical Methods in Natural Language Processing: System Demonstrations, EMNLP 2020 - Demos, Online, November 16-20, 2020*, pp. 38–45. Association for Computational Linguistics, 2020. doi: 10.18653/V1/2020.EMNLP-DEMOS.6. URL `https://doi.org/10.18653/v1/2020.emnlp-demos.6`.

Canran Xu and Ruijiang Li. Relation embedding with dihedral group in knowledge graph. In *ACL (1)*, pp. 263–272. Association for Computational Linguistics, 2019.

Haotian Xu, Yuhua Wang, and Jiahui Fan. Self-knowledge distillation for knowledge graph embedding. In *LREC/COLING*, pp. 14595–14605. ELRA and ICCL, 2024.

Bishan Yang, Wen-tau Yih, Xiaodong He, Jianfeng Gao, and Li Deng. Embedding entities and relations for learning and inference in knowledge bases. In *ICLR (Poster)*, 2015.

Shuai Zhang, Yi Tay, Lina Yao, and Qi Liu. Quaternion knowledge graph embeddings. In *NeurIPS*, pp. 2731–2741, 2019.

Wen Zhang, Chi Man Wong, Ganqiang Ye, Bo Wen, Wei Zhang, and Huajun Chen. Billion-scale pre-trained e-commerce product knowledge graph model. In *ICDE*, pp. 2476–2487. IEEE, 2021.

Yuanzhe Zhang, Kang Liu, Shizhu He, Guoliang Ji, Zhanyi Liu, Hua Wu, and Jun Zhao. Question answering over knowledge base with neural attention combining global knowledge information. *CoRR*, abs/1606.00979, 2016.

Wangchunshu Zhou, Canwen Xu, and Julian J. McAuley. BERT learns to teach: Knowledge distillation with meta learning. In Smaranda Muresan, Preslav Nakov, and Aline Villavicencio (eds.), *Proceedings of the 60th Annual Meeting of the Association for Computational Linguistics (Volume 1: Long Papers), ACL 2022, Dublin, Ireland, May 22-27, 2022*, pp. 7037–7049. Association for Computational Linguistics, 2022a. doi: 10.18653/V1/2022.ACL-LONG.485. URL `https://doi.org/10.18653/v1/2022.acl-long.485`.

Zhehui Zhou, Defang Chen, Can Wang, Yan Feng, and Chun Chen. Improving knowledge graph embedding via iterative self-semantic knowledge distillation. *CoRR*, abs/2206.02963, 2022b.

Yushan Zhu, Huaixiao Zhao, Wen Zhang, Ganqiang Ye, Hui Chen, Ningyu Zhang, and Huajun Chen. Knowledge perceived multi-modal pretraining in e-commerce. In *ACM Multimedia*, pp. 2744–2752. ACM, 2021.

Yushan Zhu, Wen Zhang, Mingyang Chen, Hui Chen, Xu Cheng, Wei Zhang, and Huajun Chen. Dualde: Dually distilling knowledge graph embedding for faster and cheaper reasoning. In *WSDM*, pp. 1516–1524. ACM, 2022.

A More Results of link prediction

More results of link prediction are shown in Table 9 and Table 10 for WN18RR, and Table 11 and Table 12 for FB15K237. All comparison results of sub-models of MED to the directly trained KGEs (DT) of 10- to 640-dimension are shown in Fig. 7.

Table 9: MRR and Hit@10 of some representative dimensions on WN18RR.

		10d		20d		40d		80d		160d		320d		640d	
	Method	*MRR*	*Hit@10*	*MRR*	*Hit@10*	*MRR*	*Hit@10*	*MRR*	*Hit@10*	*MRR*	*Hit@10*	*MRR*	*Hit@10*	*MRR*	*Hit@10*
TransE	DT	0.121	0.287	0.176	0.453	0.214	0.496	0.227	0.524	0.233	0.531	0.235	0.534	**0.237**	**0.537**
	Ext	0.125	0.298	0.172	0.423	0.199	0.468	0.213	0.495	0.225	0.515	0.226	0.521	0.237	0.537
	Ext-L	0.139	0.315	0.196	0.461	0.224	0.497	0.232	0.516	0.236	**0.534**	0.236	0.535	0.237	0.537
	Ext-V	0.139	0.309	0.198	0.458	0.222	0.494	0.234	0.525	0.236	0.532	0.236	0.536	0.237	0.537
	BKD	0.141	0.323	0.207	0.480	0.226	0.513	0.232	0.527	0.233	0.531	0.236	0.533	-	-
	TA	0.144	0.335	0.211	0.483	0.226	0.512	0.233	0.527	0.234	0.533	0.236	0.535	-	-
	DualDE	0.148	0.337	0.213	0.488	0.225	0.514	**0.234**	**0.530**	0.235	0.533	**0.238**	0.535	-	-
	IterDE	0.143	0.332	0.211	0.484	0.224	0.511	0.232	0.528	0.236	0.531	0.237	0.533	-	-
	MED	**0.170**	**0.388**	**0.219**	**0.491**	**0.232**	**0.518**	0.232	0.523	**0.236**	0.529	0.237	**0.536**	0.237	0.537
SimplE	*Method*	*MRR*	*Hit@10*	*MRR*	*Hit@10*	*MRR*	*Hit@10*	*MRR*	*Hit@10*	*MRR*	*Hit@10*	*MRR*	*Hit@10*	*MRR*	*Hit@10*
	DT	0.061	0.126	0.257	0.372	0.316	0.389	0.382	0.446	0.409	0.459	0.417	0.474	**0.421**	0.481
	Ext	0.004	0.007	0.051	0.107	0.160	0.249	0.219	0.314	0.357	0.401	0.407	0.451	0.421	0.481
	Ext-L	0.005	0.006	0.048	0.078	0.169	0.244	0.369	0.435	0.398	0.454	0.417	0.481	0.421	0.481
	Ext-V	0.004	0.006	0.047	0.076	0.246	0.317	0.368	0.402	0.398	0.461	0.413	0.472	0.421	0.481
	BKD	0.075	0.156	0.285	0.381	0.343	0.399	0.394	0.450	0.414	0.468	0.418	0.475	-	-
	TA	0.089	0.189	0.316	0.386	0.368	0.418	0.405	0.456	0.415	0.472	0.421	0.481	-	-
	DualDE	0.083	0.175	0.328	0.388	**0.386**	0.423	0.407	0.454	**0.419**	0.475	**0.422**	**0.482**	-	-
	IterDE	0.077	0.162	0.321	0.378	0.375	0.419	0.404	0.452	0.416	0.469	0.421	0.482	-	-
	MED	**0.111**	**0.224**	**0.335**	**0.395**	0.385	**0.431**	**0.407**	**0.457**	0.418	**0.477**	0.421	0.481	0.421	**0.482**
RotatE	*Method*	*MRR*	*Hit@10*	*MRR*	*Hit@10*	*MRR*	*Hit@10*	*MRR*	*Hit@10*	*MRR*	*Hit@10*	*MRR*	*Hit@10*	*MRR*	*Hit@10*
	DT	0.172	0.418	0.409	0.504	0.456	0.556	0.465	0.564	0.471	0.567	0.474	0.573	**0.476**	**0.575**
	Ext	0.299	0.378	0.379	0.464	0.437	0.516	0.458	0.544	0.467	0.549	0.471	0.552	0.476	0.575
	Ext-L	0.206	0.277	0.336	0.424	0.399	0.487	0.423	0.515	0.445	**0.541**	0.466	0.564	0.476	0.575
	Ext-V	0.261	0.377	0.304	0.433	0.337	0.471	0.366	0.497	0.416	0.532	0.451	0.561	0.476	0.575
	BKD	0.175	0.434	0.424	0.540	0.457	0.556	0.471	0.565	0.472	0.570	0.474	0.572	-	-
	TA	0.177	0.438	0.424	0.542	0.459	0.558	0.470	0.567	0.473	0.572	0.474	0.572	-	-
	DualDE	0.179	0.440	0.425	0.542	0.462	0.559	**0.471**	0.567	**0.473**	0.573	0.475	0.573	-	-
	IterDE	0.176	0.436	0.421	0.538	0.459	0.560	0.470	0.567	0.471	0.569	0.474	0.572	-	-
	MED	**0.324**	**0.469**	**0.456**	**0.543**	**0.466**	**0.561**	0.471	**0.568**	0.471	**0.574**	**0.476**	**0.573**	0.476	0.574
PairRE	*Method*	*MRR*	*Hit@10*	*MRR*	*Hit@10*	*MRR*	*Hit@10*	*MRR*	*Hit@10*	*MRR*	*Hit@10*	*MRR*	*Hit@10*	*MRR*	*Hit@10*
	DT	0.220	0.321	0.342	0.381	0.415	0.472	0.435	0.516	0.449	0.534	0.452	0.542	**0.453**	**0.544**
	Ext	0.152	0.209	0.261	0.379	0.334	0.463	0.375	0.493	0.419	0.526	0.438	0.545	0.453	0.544
	Ext-L	0.162	0.220	0.281	0.360	0.363	0.442	0.417	0.495	0.437	0.523	0.446	0.544	0.453	0.544
	Ext-V	0.172	0.260	0.306	0.374	0.389	0.456	0.420	0.498	0.441	0.529	0.446	0.541	0.453	0.544
	BKD	0.228	0.336	0.375	0.413	0.421	0.483	0.443	0.525	0.451	0.536	0.453	0.542	-	-
	TA	0.245	0.340	0.381	0.427	0.426	0.487	0.448	0.534	0.452	0.537	0.453	0.543	-	-
	DualDE	0.242	0.336	0.377	0.424	0.428	0.495	**0.451**	0.536	**0.453**	0.540	**0.454**	**0.544**	-	-
	IterDE	0.235	0.336	0.379	0.423	0.426	0.495	0.449	0.533	0.450	0.538	0.452	0.543	-	-
	MED	**0.317**	**0.376**	**0.408**	**0.467**	**0.433**	**0.502**	0.449	**0.537**	0.451	**0.541**	0.451	0.542	0.451	0.542

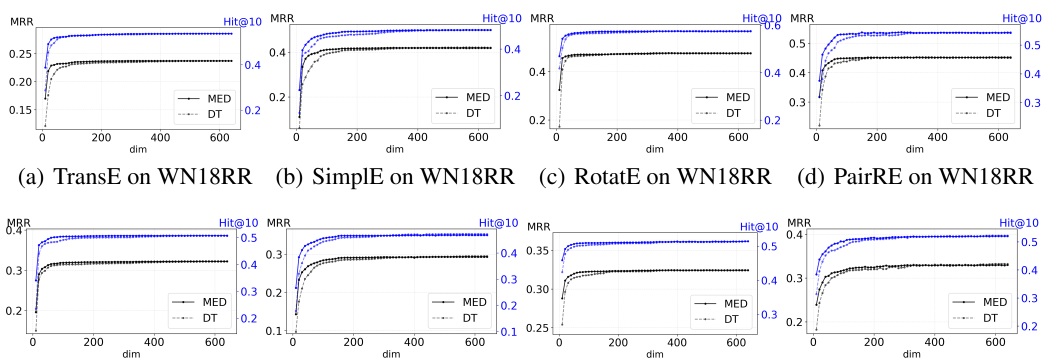

(a) TransE on WN18RR (b) SimplE on WN18RR (c) RotatE on WN18RR (d) PairRE on WN18RR

(e) TransE on FB15K237 (f) SimplE on FB15K237 (g) RotatE on FB15K237 (h) PairRE on FB15K237

Figure 7: Performance of sub-models of MED and the directly trained (DT) KGEs of dimensions from 10 to 640.

B Ablation Study

We conduct ablation studies to evaluate the effect of three modules in MED: the mutual learning mechanism (MLM), the evolutionary improvement mechanism (EIM), and the dynamic loss weight (DLW). Table 13 shows the MRR and Hit@k ($k = 1, 3, 10$) of MED removing these modules respectively on WN18RR and TransE.

Table 10: Hit@3 and Hit@1 of some representative dimensions on WN18RR.

		10d		**20d**		**40d**		**80d**		**160d**		**320d**		**640d**	
	Method	*Hit@3*	*Hit@1*	*Hit@3*	*Hit@1*	*Hit@3*	*Hit@1*	*Hit@3*	*Hit@1*	*Hit@3*	*Hit@1*	*Hit@3*	*Hit@1*	*Hit@3*	*Hit@1*
	DT	0.202	0.011	0.291	0.016	0.385	0.018	0.401	0.025	0.403	0.027	0.407	0.033	0.412	**0.034**
	Ext	0.201	0.016	0.285	0.023	0.338	0.023	0.364	0.028	0.384	0.033	0.388	0.028	0.412	0.034
	Ext-L	0.218	0.029	0.317	0.025	0.361	0.039	0.403	0.046	0.405	0.036	0.408	0.033	0.412	0.034
TransE	Ext-V	0.218	0.029	0.314	**0.045**	0.391	**0.051**	0.407	**0.047**	0.408	0.036	0.411	0.027	0.412	0.034
	BKD	0.216	0.035	0.331	0.040	0.392	0.033	0.401	0.031	0.404	0.030	0.407	0.032	-	-
	TA	0.224	0.040	0.343	0.043	0.395	0.037	0.408	0.030	0.407	0.030	0.410	0.034	-	-
	DualDE	0.226	0.037	0.346	0.043	0.394	0.037	**0.408**	0.031	**0.408**	0.031	**0.411**	**0.034**	-	-
	IterDE	0.217	0.032	0.345	0.044	0.392	0.036	0.407	0.030	0.408	0.031	0.407	0.033	-	-
	MED	**0.269**	**0.040**	**0.369**	**0.045**	**0.399**	0.038	0.404	0.042	0.407	**0.037**	0.410	0.033	**0.412**	0.031
	Method	*Hit@3*	*Hit@1*	*Hit@3*	*Hit@1*	*Hit@3*	*Hit@1*	*Hit@3*	*Hit@1*	*Hit@3*	*Hit@1*	*Hit@3*	*Hit@1*	*Hit@3*	*Hit@1*
	DT	0.061	0.028	0.297	0.193	0.361	0.289	0.406	0.343	0.420	0.382	0.428	0.386	0.433	**0.391**
	Ext	0.003	0.001	0.055	0.023	0.181	0.114	0.249	0.168	0.377	0.329	0.422	0.381	0.433	0.391
	Ext-L	0.004	0.003	0.051	0.031	0.187	0.128	0.389	0.333	0.413	0.365	0.429	0.384	0.433	0.391
SimplE	Ext-V	0.004	0.002	0.050	0.029	0.269	0.205	0.378	0.349	0.409	0.372	0.426	0.382	0.433	0.391
	BKD	0.077	0.034	0.331	0.225	0.384	0.311	0.415	0.358	0.426	0.371	0.431	0.385	-	-
	TA	0.093	0.042	0.349	0.269	0.375	0.349	0.412	**0.384**	0.425	0.388	0.431	0.389	-	-
	DualDE	0.086	0.038	0.361	0.285	0.391	**0.368**	0.416	0.383	0.427	**0.389**	0.434	**0.392**	-	-
	IterDE	0.079	0.033	0.355	0.279	0.382	0.356	0.415	0.379	0.424	0.383	0.433	0.389	**-**	**-**
	MED	**0.119**	**0.048**	**0.366**	**0.292**	**0.395**	0.359	**0.419**	0.380	**0.429**	0.389	**0.435**	0.391	**0.434**	0.390
	Method	*Hit@3*	*Hit@1*	*Hit@3*	*Hit@1*	*Hit@3*	*Hit@1*	*Hit@3*	*Hit@1*	*Hit@3*	*Hit@1*	*Hit@3*	*Hit@1*	*Hit@3*	*Hit@1*
	DT	0.304	0.005	0.436	0.357	0.475	0.393	0.487	0.420	0.489	0.423	0.491	0.428	0.493	**0.429**
	Ext	0.315	0.257	0.399	0.335	0.452	0.395	0.472	0.415	0.480	0.413	0.470	0.418	0.493	0.429
	Ext-L	0.224	0.166	0.359	0.288	0.420	0.352	0.441	0.373	0.461	0.396	0.481	0.417	0.493	0.429
RotatE	Ext-V	0.289	0.197	0.336	0.234	0.377	0.263	0.402	0.293	0.442	0.357	0.467	0.397	0.493	0.429
	BKD	0.312	0.009	0.452	0.361	0.479	0.403	0.487	0.421	0.490	0.424	0.492	0.425	-	-
	TA	0.314	0.010	0.452	0.363	0.481	0.408	0.489	0.420	0.488	0.422	0.492	0.425	-	-
	DualDE	0.320	0.011	0.452	0.364	0.483	0.412	0.489	**0.423**	0.488	**0.426**	0.491	0.425	-	-
	IterDE	0.311	0.013	0.439	0.356	0.479	0.407	0.484	0.423	0.488	0.425	0.493	0.424	-	-
	MED	**0.354**	**0.277**	**0.476**	**0.409**	**0.486**	**0.418**	**0.490**	0.422	**0.492**	0.424	**0.493**	**0.427**	**0.495**	0.428
	Method	*Hit@3*	*Hit@1*	*Hit@3*	*Hit@1*	*Hit@3*	*Hit@1*	*Hit@3*	*Hit@1*	*Hit@3*	*Hit@1*	*Hit@3*	*Hit@1*	*Hit@3*	*Hit@1*
	DT	0.271	,0.174	0.368	0.313	0.428	0.384	0.450	0.399	0.463	0.405	0.462	0.406	**0.464**	**0.407**
	Ext	0.163	0.120	0.292	0.198	0.366	0.267	0.398	0.314	0.437	0.364	0.452	0.388	0.464	0.407
	Ext-L	0.175	0.129	0.302	0.237	0.383	0.319	0.431	0.377	0.450	0.395	0.455	0.400	0.464	0.407
PairRE	Ext-V	0.192	0.124	0.323	0.269	0.407	0.352	0.435	0.379	0.452	0.398	0.458	0.400	0.464	0.407
	BKD	0.279	0.184	0.388	0.334	0.435	0.372	0.452	0.405	0.460	0.405	0.463	0.407	-	-
	TA	0.293	0.197	0.387	0.332	0.437	0.380	0.460	0.404	0.462	0.409	0.463	0.408	-	-
	DualDE	0.281	0.175	0.389	0.330	0.437	0.381	**0.463**	**0.409**	0.463	0.410	0.465	**0.410**	-	-
	IterDE	0.285	0.172	0.390	0.331	0.435	0.377	0.461	0.405	0.463	**0.411**	0.464	0.410	-	-
	MED	**0.314**	**0.259**	**0.426**	**0.367**	**0.443**	**0.392**	0.462	0.405	**0.464**	0.406	**0.465**	0.407	0.464	0.406

Table 11: MRR and Hit@10 of some representative dimensions on FB15K237.

		10d		**20d**		**40d**		**80d**		**160d**		**320d**		**640d**	
TransE	*Method*	*MRR*	*Hit@10*	*MRR*	*Hit@10*	*MRR*	*Hit@10*	*MRR*	*Hit@10*	*MRR*	*Hit@10*	*MRR*	*Hit@10*	*MRR*	*Hit@10*
	DT	0.150	0.235	0.277	0.440	0.299	0.477	0.313	0.484	0.315	0.499	0.318	0.501	0.322	**0.508**
	Ext	0.115	0.211	0.191	0.324	0.236	0.392	0.266	0.436	0.286	0.462	0.299	0.479	0.322	0.508
	Ext-L	0.109	0.194	0.175	0.293	0.232	0.381	0.263	0.424	0.285	**0.462**	0.301	0.484	0.322	0.508
	Ext-V	0.139	0.256	0.200	0.348	0.237	0.396	0.270	0.437	0.293	0.466	0.308	0.488	0.322	0.508
	BKD	0.176	0.293	0.279	0.446	0.303	0.480	0.315	0.500	0.315	0.501	0.320	0.502	-	-
	TA	0.175	0.246	0.281	0.441	0.303	0.484	0.314	0.498	0.319	0.504	0.321	0.504	-	-
	DualDE	0.179	0.301	0.281	0.443	0.306	0.483	0.316	0.502	0.319	0.505	**0.322**	**0.508**	-	-
	IterDE	0.176	0.285	0.276	0.446	0.307	0.482	0.315	**0.503**	0.317	0.505	0.319	0.505	-	-
	MED	**0.196**	**0.341**	**0.290**	**0.472**	**0.308**	**0.486**	**0.317**	0.502	**0.320**	**0.505**	0.321	0.507	**0.322**	0.507
SimplE	*Method*	*MRR*	*Hit@10*	*MRR*	*Hit@10*	*MRR*	*Hit@10*	*MRR*	*Hit@10*	*MRR*	*Hit@10*	*MRR*	*Hit@10*	*MRR*	*Hit@10*
	DT	0.097	0.179	0.176	0.321	0.236	0.390	0.271	0.431	0.285	0.458	0.291	0.467	**0.295**	**0.472**
	Ext	0.037	0.068	0.069	0.107	0.090	0.144	0.159	0.258	0.229	0.372	0.269	0.432	0.295	0.472
	Ext-L	0.045	0.059	0.056	0.062	0.083	0.146	0.114	0.205	0.196	0.316	0.258	0.421	0.295	0.472
	Ext-V	0.049	0.069	0.066	0.101	0.105	0.149	0.138	0.224	0.224	0.369	0.261	0.414	0.295	0.472
	BKD	0.113	0.204	0.182	0.315	0.244	0.412	0.275	0.439	0.287	0.463	0.293	0.470	-	-
	TA	0.124	0.221	0.192	0.329	0.254	0.416	0.276	0.448	0.290	0.465	0.295	0.471	-	-
	DualDE	0.120	0.213	0.195	0.346	0.258	**0.429**	0.279	0.443	**0.293**	0.466	**0.296**	**0.468**	-	-
	IterDE	0.120	0.215	0.193	0.338	0.257	0.427	0.281	0.440	0.293	0.465	0.297	0.468	-	-
	MED	**0.143**	**0.267**	**0.233**	**0.384**	**0.261**	0.427	**0.279**	**0.448**	0.291	**0.466**	0.293	0.468	0.294	0.470
RotatE	*Method*	*MRR*	*Hit@10*	*MRR*	*Hit@10*	*MRR*	*Hit@10*	*MRR*	*Hit@10*	*MRR*	*Hit@10*	*MRR*	*Hit@10*	*MRR*	*Hit@10*
	DT	0.254	0.424	0.297	0.477	0.312	0.495	0.317	0.502	0.322	0.506	0.323	0.510	**0.325**	**0.515**
	Ext	0.138	0.245	0.203	0.340	0.251	0.410	0.276	0.443	0.291	0.465	0.305	0.485	0.325	0.515
	Ext-L	0.135	0.243	0.188	0.319	0.221	0.365	0.246	0.402	0.280	0.453	0.299	0.477	0.325	0.515
	Ext-V	0.160	0.281	0.198	0.340	0.238	0.393	0.265	0.427	0.288	0.458	0.302	0.478	0.325	0.515
	BKD	0.277	0.442	0.305	0.485	0.314	0.503	0.321	0.508	0.322	0.510	0.323	0.509	-	-
	TA	0.280	0.447	0.306	0.485	0.313	0.501	0.319	0.507	0.323	0.510	0.323	0.509	-	-
	DualDE	0.282	0.449	0.307	0.486	0.315	0.502	0.318	0.507	0.322	**0.512**	0.324	**0.514**	-	-
	IterDE	0.276	0.445	0.306	0.482	0.317	0.504	0.319	0.508	0.323	0.512	0.324	0.513	-	-
	MED	**0.288**	**0.459**	**0.311**	**0.492**	**0.318**	**0.504**	**0.322**	**0.509**	**0.323**	0.510	**0.324**	0.512	0.324	0.514
PairRE	*Method*	*MRR*	*Hit@10*	*MRR*	*Hit@10*	*MRR*	*Hit@10*	*MRR*	*Hit@10*	*MRR*	*Hit@10*	*MRR*	*Hit@10*	*MRR*	*Hit@10*
	DT	0.182	0.314	0.243	0.395	0.284	0.452	0.307	0.476	0.319	0.505	0.328	0.518	**0.332**	**0.522**
	Ext	0.148	0.222	0.177	0.289	0.217	0.353	0.259	0.416	0.294	0.469	0.321	0.506	0.332	0.522
	Ext-L	0.150	0.249	0.196	0.294	0.219	0.333	0.271	0.436	0.309	0.489	0.326	0.513	0.332	0.522
	Ext-V	0.176	0.277	0.192	0.303	0.229	0.374	0.279	0.450	0.311	0.490	0.329	0.513	0.332	0.522
	BKD	0.198	0.332	0.251	0.407	0.288	0.453	0.311	0.487	0.321	0.508	0.330	0.521	-	-
	TA	0.208	0.346	0.263	0.430	0.292	0.455	0.314	0.493	0.323	0.509	0.332	0.521	-	-
	DualDE	0.207	0.342	0.261	0.427	0.293	0.456	**0.316**	0.495	**0.326**	**0.512**	**0.334**	**0.524**	-	-
	IterDE	0.205	0.340	0.264	0.431	0.293	0.462	0.314	0.494	0.324	0.508	0.332	0.522	-	-
	MED	**0.239**	**0.384**	**0.274**	**0.437**	**0.303**	**0.466**	0.314	**0.495**	0.324	0.510	0.329	0.521	0.330	0.520

B.1 Mutual Learning Mechanism (MLM)

We remove the mutual learning mechanism from MED and keep the other parts unchanged, where equation 6 is rewritten as

$$L = \sum_{i=1}^{n} \exp\left(\frac{w_3 \cdot d_i}{d_n}\right) \cdot L_{EI}^{i}. \tag{7}$$

From the result of "MED w/o MLM" in Table 13, we find that after removing the mutual learning mechanism, the performance of low-dimensional sub-models deteriorates seriously since the low-dimensional sub-models can not learn from the high-dimensional sub-models. For example, the MRR of the 10-dimensional sub-model decreased by 12.4%, and the MRR of the 20-dimensional sub-model decreased by 10%. While the performance degradation of the high-dimensional sub-model is not particularly obvious, and the MRR of the highest-dimensional sub-model ($dim = 640$) is not worse than that of MED, which is because to a certain degree, removing the mutual learning mechanism also avoids the negative influence to high-dimensional sub-models from low-dimensional sub-models. On the whole, this mechanism greatly improves the performance of low-dimensional sub-models.

B.2 Evolutionary Improvement Mechanism (EIM)

In this part, we replace evolutionary improvement loss L_{EI}^{i} in equation 6 with the regular KGE loss L_{KGE}^{i}:

$$L_{KGE}^{i} = \sum_{(h,r,t)\in\mathcal{T}\cup\mathcal{T}^{-}} y \log \sigma(s_{(h,r,t)}^{i}) + (1-y)\log(1-\sigma(s_{(h,r,t)}^{i})). \tag{8}$$

From the result of "MED w/o EIM" in Table 13, we find that removing the evolutionary improvement mechanism mainly degrades the performance of high-dimensional sub-models. While due to the

Table 12: Hit@3 and Hit@1 of some representative dimensions on FB15K237.

		10d		20d		40d		80d		160d		320d		640d	
	Method	*Hit@3*	*Hit@1*	*Hit@3*	*Hit@1*	*Hit@3*	*Hit@1*	*Hit@3*	*Hit@1*	*Hit@3*	*Hit@1*	*Hit@3*	*Hit@1*	*Hit@3*	*Hit@1*
TransE	DT	0.169	0.102	0.301	0.190	0.327	0.212	0.340	0.218	0.348	0.222	0.353	0.224	**0.358**	**0.228**
	Ext	0.123	0.065	0.211	0.122	0.264	0.156	0.296	0.180	0.320	0.197	0.331	0.208	0.358	0.228
	Ext-L	0.118	0.065	0.192	0.115	0.256	0.157	0.292	0.180	0.316	0.198	0.333	0.210	0.358	0.228
	Ext-V	0.150	0.081	0.222	0.126	0.265	0.156	0.301	0.185	0.325	0.205	0.341	0.217	0.358	0.228
	BKD	0.178	0.106	0.308	0.198	0.336	0.208	0.349	0.222	0.349	0.223	0.354	0.226	-	-
	TA	0.188	0.112	0.307	0.200	0.336	0.212	0.348	0.220	0.353	0.225	0.355	0.223	-	-
	DualDE	0.193	0.115	0.307	**0.201**	0.337	0.216	**0.351**	0.223	**0.354**	0.226	0.356	0.227	-	-
	IterDE	0.187	0.112	0.299	0.185	0.333	0.214	0.351	0.222	0.353	0.223	0.354	0.224	-	-
	MED	**0.215**	**0.122**	**0.321**	0.199	**0.338**	**0.218**	0.347	**0.223**	0.351	**0.226**	**0.356**	**0.227**	0.358	0.227
	Method	*Hit@3*	*Hit@1*	*Hit@3*	*Hit@1*	*Hit@3*	*Hit@1*	*Hit@3*	*Hit@1*	*Hit@3*	*Hit@1*	*Hit@3*	*Hit@1*	*Hit@3*	*Hit@1*
SimplE	DT	0.103	0.055	0.193	0.105	0.256	0.161	0.297	0.191	0.314	0.197	0.323	0.208	**0.324**	**0.211**
	Ext	0.039	0.019	0.071	0.047	0.091	0.057	0.171	0.109	0.251	0.159	0.294	0.187	0.324	0.211
	Ext-L	0.043	0.035	0.048	0.037	0.111	0.040	0.131	0.093	0.216	0.134	0.281	0.177	0.324	0.211
	Ext-V	0.047	0.036	0.074	0.043	0.097	0.077	0.145	0.109	0.248	0.156	0.289	0.189	0.324	0.211
	BKD	0.123	0.064	0.201	0.115	0.261	0.164	0.299	0.191	0.308	0.202	0.318	**0.213**	-	-
	TA	0.133	0.073	0.210	0.123	0.276	0.175	0.302	0.195	0.318	0.203	0.323	0.211	-	-
	DualDE	0.130	0.071	0.224	0.115	0.279	0.175	0.305	0.196	0.324	**0.208**	**0.326**	0.211	-	-
	IterDE	0.132	0.069	0.217	0.118	0.276	0.174	0.303	0.192	**0.326**	0.204	0.324	0.212	-	-
	MED	**0.164**	**0.073**	**0.254**	**0.158**	**0.288**	**0.177**	**0.305**	**0.196**	0.319	0.205	0.318	0.209	0.322	0.209
	Method	*Hit@3*	*Hit@1*	*Hit@3*	*Hit@1*	*Hit@3*	*Hit@1*	*Hit@3*	*Hit@1*	*Hit@3*	*Hit@1*	*Hit@3*	*Hit@1*	*Hit@3*	*Hit@1*
RotatE	DT	0.284	0.168	0.330	0.207	0.346	0.223	0.352	0.224	0.353	0.229	0.357	0.230	**0.363**	**0.234**
	Ext	0.152	0.080	0.225	0.129	0.278	0.170	0.304	0.190	0.322	0.203	0.335	0.217	0.363	0.234
	Ext-L	0.147	0.078	0.209	0.121	0.247	0.146	0.275	0.166	0.312	0.193	0.333	0.209	0.363	0.234
	Ext-V	0.174	0.097	0.218	0.126	0.264	0.159	0.293	0.182	0.319	0.201	0.336	0.213	0.363	0.234
	BKD	0.306	0.193	0.338	0.214	0.352	0.224	0.354	0.230	0.356	0.230	0.358	0.231	-	-
	TA	0.308	0.196	0.339	0.216	0.353	0.225	0.358	0.229	0.359	0.229	0.358	0.231	-	-
	DualDE	0.311	0.197	0.341	0.216	0.353	**0.227**	**0.360**	0.230	0.361	0.232	0.361	0.233	-	-
	IterDE	0.307	0.195	0.342	0.215	0.355	0.225	0.359	**0.232**	**0.363**	0.233	0.362	**0.234**	-	-
	MED	**0.324**	**0.201**	**0.344**	**0.216**	**0.355**	0.225	0.357	0.231	0.358	**0.233**	**0.362**	0.233	0.362	0.232
	Method	*Hit@3*	*Hit@1*	*Hit@3*	*Hit@1*	*Hit@3*	*Hit@1*	*Hit@3*	*Hit@1*	*Hit@3*	*Hit@1*	*Hit@3*	*Hit@1*	*Hit@3*	*Hit@1*
PairRE	DT	0.198	0.116	0.262	0.162	0.312	0.202	0.337	0.222	0.352	0.227	0.364	0.235	**0.368**	**0.237**
	Ext	0.158	0.107	0.187	0.118	0.236	0.149	0.283	0.182	0.325	0.207	0.354	0.230	0.368	0.237
	Ext-L	0.159	0.099	0.196	0.134	0.238	0.159	0.298	0.188	0.342	0.219	0.359	0.233	0.368	0.237
	Ext-V	0.181	0.116	0.192	0.125	0.250	0.154	0.307	0.193	0.343	0.221	0.362	0.237	0.368	0.237
	BKD	0.215	0.132	0.265	0.168	0.314	0.203	0.343	0.224	0.355	0.233	0.366	0.236	-	-
	TA	0.226	0.139	0.291	0.182	0.316	0.210	0.347	0.224	0.358	0.232	0.368	0.235	-	-
	DualDE	0.224	0.139	0.286	0.179	0.318	0.212	0.351	0.226	**0.359**	**0.234**	**0.371**	**0.238**	-	-
	IterDE	0.225	0.135	0.293	0.185	0.324	0.212	**0.352**	0.224	0.357	0.234	0.369	0.236	-	-
	MED	**0.253**	**0.172**	**0.299**	**0.189**	**0.327**	**0.213**	0.346	**0.224**	0.357	0.232	0.366	0.236	0.368	0.235

Table 13: Ablation study on WN18RR with TransE.

dim	MED				MED w/o MLM				MED w/o EIM				MED w/o DLW			
	MRR	*Hit@10*	*Hit@3*	*Hit@1*	*MRR*	*Hit@10*	*Hit@3*	*Hit@1*	*MRR*	*Hit@10*	*Hit@3*	*Hit@1*	*MRR*	*Hit@10*	*Hit@3*	*Hit@1*
10	.170	**.388**	**.269**	.036	.149	.335	.234	.032	.169	.388	.267	**.037**	**.171**	.387	.268	.035
20	**.219**	**.491**	**.369**	.042	.197	.437	.323	.032	.217	.488	.366	**.044**	.218	.487	.367	.039
40	**.232**	**.518**	.399	**.048**	.224	.496	.379	.029	.232	.517	**.403**	.042	.232	.517	.402	.037
80	.232	.523	.404	**.042**	.228	.521	.399	.033	**.235**	**.529**	.408	.037	.234	.523	**.410**	.041
160	**.236**	**.529**	**.407**	**.037**	.234	.525	.406	.034	.234	.527	.405	.032	.235	.527	.405	.032
320	**.237**	**.536**	**.410**	.033	.236	.532	.409	**.035**	.233	.530	.398	.031	.234	.533	.405	.029
640	.237	**.537**	**.412**	.031	**.238**	.535	.412	**.042**	.232	.528	.402	.029	.233	.530	.396	.025

existence of the mutual learning mechanism, the low-dimensional sub-model can still learn from the high-dimensional sub-model, so as to ensure the certain performance of the low-dimensional sub-model. In addition, we also find that as the dimension increases to a certain extent, the performance of the sub-model does not improve, and even begins to decline. We guess that this is because the mutual learning mechanism makes every pair of neighbor sub-models learn from each other, resulting in some low-quality or wrong knowledge gradually transferring from the low-dimensional sub-models to the high-dimensional sub-models, and when the evolutionary improvement mechanism is removed, the high-dimensional sub-models can no longer correct the wrong information from the low-dimensional sub-models. The higher the dimension of the sub-model, the more the accumulated error, so the performance of the high-dimensional sub-models is seriously damaged. On the whole, this mechanism mainly helps to improve the effect of high-dimensional sub-models.

B.3 DYNAMIC LOSS WEIGHT (DLW)

To study the effect of the dynamic loss weight, we fix the ratio of all mutual learning losses to all evolutionary improvement losses as $1:1$, and equation 6 is rewritten as

$$L = \sum_{i=2}^{n} L_{ML}^{i-1,i} + \sum_{i=1}^{n} L_{EI}^{i}. \tag{9}$$

According to the result of "MED w/o DLW" in Table 13, the overall results of "MED w/o DLW" are in the middle of the results of "MED w/o MLM" and "MED w/o EIM": the performance of the low-dimensional sub-model is better than that of "MED w/o MLM", and the performance of the high-dimensional sub-model is better than that of "MED w/o EIM". On the whole, its results are more similar to "MED w/o EIM", that is, the performance of the low-dimensional sub-model does not change much, while the performance of the high-dimensional sub-model decreases more significantly. We believe that for the high-dimensional sub-model, the proportion of mutual learning loss is still too large, which makes it more negatively affected by the low-dimensional sub-model. This result indicates that the dynamic loss weight plays a role in adaptively balancing multiple losses and contributes to improving overall performance.

C DETAILS OF APPLYING THE TRAINED KGE BY MED TO REAL APPLICATIONS

The SKG is used in many tasks related to users, and injecting user embeddings trained over SKG into downstream task models is a common and practical way.

User labeling is one of the common user management tasks that e-commerce platforms run on backend servers. We model user labeling as a multiclass classification task for user embeddings with a 2-layer MLP:

$$\mathcal{L} = -\frac{1}{|\mathcal{U}|} \sum_{i=1}^{|\mathcal{U}|} \sum_{j=1}^{|\mathcal{CLS}|} y_{ij} \log(\mathrm{MLP}(u_i)), \tag{10}$$

where u_i is the i-th user's embedding, the label $y_{ij} = 1$ if user u_i belongs to class cls_j, otherwise $y_{ij} = 0$.

The product recommendation task is to properly recommend items to users that users will interact with a high probability and it often runs on terminal devices. Following PKGM Zhang et al. (2021), which recommends items to users using the neural collaborative filtering (NCF) He et al. (2017) framework with the help of pre-trained user embeddings as service vectors, we add trained user embeddings over SKG as service vectors to NCF. In NCF, the MLP layer is used to learn item-user interactions based on the latent feature of the user and item, that is, for a given user-item pair $user_i - item_j$, the interaction function is

$$\phi_1^{MLP}(p_i, q_j) = \mathrm{MLP}([p_i; q_j]), \tag{11}$$

where p_i and q_j are latent feature vectors of user and item learned in NCF. We add the trained user embedding u_i to NCF's MLP layer and rewrite Equation equation 11 as

$$\phi_1^{MLP}(p_i, q_j, u_i) = \mathrm{MLP}([p_i; q_j; u_i]), \tag{12}$$

and the other parts of NCF stay the same as in PKGM Zhang et al. (2021).

We train entity and relation embeddings for SKG based on TransE Bordes et al. (2013) and input the trained entity (user) embedding into Equation equation 10 and Equation equation 12.

D Details of extending MED to language model BERT-base

D.1 Dataset and Evaluation Metric

For the experiments extending MED to BERT, we adopt the common GLUE Wang et al. (2019) benchmark for evaluation. To be specific, we use the development set of the GLUE benchmark which includes four tasks: Paraphrase Similarity Matching, Sentiment Classification, Natural Language Inference, and Linguistic Acceptability. For Paraphrase Similarity Matching, we use MRPC Dolan & Brockett (2005), QQP and STS-B Conneau & Kiela (2018) for evaluation. For Sentiment Classification, we use SST-2 Socher et al. (2013). For Natural Language Inference, we use MNLI Williams et al. (2018), QNLI Rajpurkar et al. (2016), and RTE for evaluation. In terms of evaluation metrics, we follow previous work Devlin et al. (2019); Sun et al. (2019a). For MRPC and QQP, we report F1 and accuracy. For STS-B, we consider Pearson and Spearman correlation as our metrics. The other tasks use accuracy as the metric. For MNLI, the results of MNLI-m and MNLI-mm are both reported separately.

D.2 Baselines

For comparison, we choose Knowledge Distillation (KD) models and Hardware-Aware Transformers Wang et al. (2020a) (HAT) customized for transformers as baselines. For the KD models, we compare MED with Basic KD (BKD) Hinton et al. (2015), Patient KD (PKD) Sun et al. (2019a), Relational Knowledge Distillation (RKD) Park et al. (2019), Deep Self-attention Distillation (MiniLM) Wang et al. (2020b), Meta Learning-based KD (MetaDistill) Zhou et al. (2022a) and Feature Structure Distillation (FSD) Jung et al. (2023). For the comparability of the results, we choose 4-layer BERT (BERT_4) or 6-layer BERT (BERT_6) as the student model architectures, which guarantees that the number of model parameters (*#P(M)*) or *speedup* is comparable. For HAT, we use the same model architecture as our MED for training and show the results of sub-models with three parameter scales.

D.3 Implementation

To implement MED on BERT, for the word embedding layer, all sub-models share the front portion of embedding parameters in the same way as in KGE, and for the transformer layer, all sub-models share the front portion of weight parameters as in HAT Wang et al. (2020a). Specifically, assuming that the embedding dimension of the largest BERT model B_n is d_n, and the embedding dimension of the sub-model B_i is d_i, for any parameter matrix with the shape $x \times y$ in B_n, the front portion sub-matrix of it with the shape $\frac{d_i}{d_n}x \times \frac{d_i}{d_n}y$ is the parameter matrix of the corresponding position in B_i. Finally, it just need to replace the triple score $s_{(h,r,t)}$ in Equation equation 2, Equation equation 3, Equation equation 4, and Equation equation 5 with the logits output for the corresponding category of the classifier in the classification task.

We set $n = 4$ for BERT applying MED, and 4 sub-models have the following settings: [768, 512, 256, 128] for embedding dim and [768, 512, 256, 128] for hidden dim, [12, 12, 6, 6] for the head number in attention modules, 12 for encoder layer number.